




Article

Migration Features and Regularities of Heavy Metals Transformation in Fresh and Marine Ecosystems (Peter the Great Bay and Lake Khanka)

Eduard Tokar' ¹, Natalia Kuzmenkova ^{2,*}, Alexandra Rozhkova ², Andrey Egorin ¹, Daria Shlyk ¹, Keliang Shi ³, Xiaolin Hou ³ and Stepan Kalmykov ²

¹ Institute of Chemistry, Far Eastern Branch, Russian Academy of Sciences, 159, Prosp. 100-Letya Vladivostoka, Vladivostok 690022, Russia; d.edd@mail.ru (E.T.); andrey.egorin@gmail.com (A.E.); daria79@list.ru (D.S.)

² Department of Chemistry, Lomonosov Moscow State University, 1 Bld. 3, Leninskie Gory, Moscow 119991, Russia; rozhkova@radiomsu.ru (A.R.); stepan@radio.chem.msu.ru (S.K.)

³ School of Nuclear Science and Technology, Lanzhou University, Lanzhou 730000, China; shikl@lzu.edu.cn (K.S.); houxl@lzu.edu.cn (X.H.)

* Correspondence: kuzmenkovanv@my.msu.ru

Abstract: Peter the Great Bay and Lake Khanka are among the most important structural and industrial fishing parts of the Far East coastal ecosystem, which are used by a number of countries such as Russia, China, Korea, Japan, etc. At the same time, the active use of water resources, as well as industrial activities deployed on the coastal part of these reservoirs, are accompanied by a constant flow of pollutants into the water area. Among them, one can include heavy metals; their entry and migration are currently not fully controlled. There exists an important scientific and ecological task to study the features of heavy metal migration and transformation in natural objects. Bottom sediments act as a substrate for hydrobionts and, at the same time, serve as accumulators of pollutants, so that they can be used as the main component of the coastal-shelf ecosystem. The geochemical assessment of the behavior of heavy metals in the bottom sediments of Ussuri Bay and Amur Bay (Sea of Japan) and Lake Khanka (Xingkai) has been performed. Qualitative and quantitative elemental compositions of the bottom sediments have been established by means of the inductively coupled plasma-mass spectrometry (ICP-MS), atomic absorption spectrometry (AAS), and X-ray fluorescence analysis (XRF), whereas a correlation with the concentration of elements in seawater above sediments has been provided. The main phases of anthropogenic components as well as their relationship with an increased content of heavy metals have been established using X-ray diffraction analysis (XRD). Average values of the concentration of elements in the bottom sediments of Peter the Great Bay decrease in the following row: Fe > Cu > Cr > Zn ≥ Pb > Mn > Ni, and for Lake Khanka: Pb > Cu > Mn > Fe > Cr > Zn > Ni. Here, the excessive contents of Cr, Fe, Cu, Zn, and Pb in sea bottom sediments by 6, 32, 7, 3, and 4 times as compared with background values are the result of the formation of a large amount of carbonate and iron-oxide phases. At the same time, it was shown that, during the transition from the estuarine (coastal) area of river flow to the central (closer to the outlet to the ocean), the concentration of biogenic metals (Ni, Zn, Pb, Cu) generally decreased 2–4-fold along the profile, which was associated with the formation of their hydroxides and carbonates in the area of mixing of freshwater and seawater followed by that of complex compounds or absorption. A significant anthropogenic impact is observed in the lake sediments, which is demonstrated by the excess of Pb concentration by 6700 times, as compared with the Clarke number of the lithosphere. The non-uniform distribution of heavy metals along the core profile has been established, which is related to different contents of aluminosilicate and iron oxide phases in the form of hematite and magnetite. The sedimentation rate has been established by means of granulometric and radiometric analysis and equaled to 0.45 mm/year in Ussuri Bay, 1.6 mm/year in Amur Bay, and 0.43–0.50 mm/year in Lake Khanka. By calculating the distribution coefficients of heavy metals in the 'water–deposits' system, some features of migration and accumulation of individual elements have been established. To assess the potential pollution of the marine areas, the geoaccumulation index (Igeo) and the pollution factor (Kc) have been calculated. In comparison with the maximum



Citation: Tokar', E.; Kuzmenkova, N.; Rozhkova, A.; Egorin, A.; Shlyk, D.; Shi, K.; Hou, X.; Kalmykov, S. Migration Features and Regularities of Heavy Metals Transformation in Fresh and Marine Ecosystems (Peter the Great Bay and Lake Khanka). *Water* **2023**, *15*, 2267. <https://doi.org/10.3390/w15122267>

Academic Editor: Lydia Bondareva

Received: 14 May 2023

Revised: 14 June 2023

Accepted: 14 June 2023

Published: 17 June 2023



Copyright: © 2023 by the authors. Licensee MDPI, Basel, Switzerland. This article is an open access article distributed under the terms and conditions of the Creative Commons Attribution (CC BY) license (<https://creativecommons.org/licenses/by/4.0/>).

permissible concentrations of the Russian Federation (MPC), the World Health Organization (WHO), the US Environmental Protection Agency (US EPA), and environmental protection agencies of China and Japan, Peter the Great Bay has an excess of Mn—2-fold, Fe—2-fold, Zn—3-fold, whereas in Lake Khanka, the situation is even less favorable, in particular, the excess of Mn is 79-fold, Fe—35-fold, Cu—2-fold, Zn—3–4-fold, which is clearly determined by the closeness of the water basin and the lack of water exchange. In comparison with the lithosphere Clarke number, the sediments of both water basins, as well as the coastal soil of the lake, are enriched with Pb and depleted with Cr, Ni, and Zn. The highest values of Igeo in both water basins have been observed for Pb, and equaled 12–16 in Peter the Great Bay and 6000 in Khanka Lake. Based on the data obtained, the areas with the greatest pollution caused by natural and anthropogenic factors have been identified.

Keywords: heavy metals; Far East region; fresh and marine ecosystems; pollution; sediment analysis; bottom sediments

1. Introduction

Pollution of the biosphere by heavy metals (HM) as a result of anthropogenic activities poses a danger to the ecosystem and to humanity. The problem of HM pollution is most serious in the territories used for agriculture, as well as coastal zones with active economic operations related to mariculture harvesting.

A majority of all pollutants, including HMs, enter water bodies with continental runoff and subsequent migration along trophic chains [1,2]. Here, some HMs are characterized by biomagnification in living organisms [3–5], while most HMs do not accumulate there [6,7] and ultimately are deposited in sea bottom sediments [8,9] of freshwater basins (ponds, lakes) and coastal sea areas. Here, the migration of heavy metals in water basins directly depends on the magnitude of the distribution coefficient in the ‘water–bottom sediments (BS)’ system [8]. In the processes of transfer and deposition of BS, HM adsorbed on them are exposed to all physical–chemical and biological processes occurring in an aqueous environment with significant seasonal changes [10]. In an equilibrium medium, sedimentation of suspended matter occurs; however, as a result of dynamic changes in equilibrium under the action of bioturbation, as well as natural and anthropogenic physical chemical processes, a secondary transition of accumulated elements into a water-soluble form is possible [11]. In addition, suspended particles are actively transported by water currents, which contributes to the redistribution of pollutants in large water areas. The study of the HM content in bottom sediments of various types of water basins at the interface of the water/sediment phases, as well as along vertical profiles of BS, can serve as an integral indicator of the degree of pollution of water bodies and enables one to evaluate and establish the mechanisms of migration of elements [12–15].

The study of the migration and transformation of HM in seawater and freshwater basins of the same geographical region is of particular interest due to the various effects of natural conditions and pollution sources, which are the fundamental factors of migration and concentration of HM in bottom sediments.

Peter the Great Bay is one of the most important structural, functional, and fishing parts of the coastal ecosystem of the Sea of Japan due to its vast water area, bays of different sizes, and substantially long coastline with a developed industrial infrastructure. The highest urbanization rate of the coastal territory is observed around Ussuri Bay and Amur Bay, which are the largest inland water basins occupying the northeastern part of the Bay and which wash the shores of the city of Vladivostok. The length of the coastline of both water basins varies between 50 and 60 km, whereas the maximum depth is 50–60 m. Only some parts of the wastewater from residential areas and industrial facilities of the city of Vladivostok are processed at treatment facilities. The greatest damage is caused by the enterprises of water and communal services. According to the estimates of the Unified State System of Information on the Situation in the World Ocean maintained in Russia,

their share in wastewater discharged into Peter the Great Bay is 55%, in Amur Bay—72%, and in Ussuri Bay—49%. The damage of substances formed from fish processing and agricultural activities that have toxic properties in Peter the Great Bay accounts for 28%. The yearly influx of pollutants into the internal bays of Peter the Great Bay is 4.82 g/m³ of seawater in Amur Bay, and 269.2 g/m³ in Zolotoy Rog Bay. According to expert estimates, the actual volumes of annual releases of certain pollutants into the waters of the bay are many times higher than the corresponding estimates of state statistical reports. Therefore, at analyzing the state and causes of pollution of water areas, it is necessary not only to consider the volume of wastewater or other pollutants, but also to critically approach the information itself. The coastline of Amur Bay formed by islands, shallow spits, and sand bars contributes to the formation of heterogeneous hydrological conditions, which is reflected in the sedimentogenesis of the bay. The largest river in the south of Primorsky Krai (Razdolnaya River) flows into the upper part of Amur Bay, the waters of which are carried into the bay by municipal wastewater from the cities of Suifenhe (PRC), Ussuriysk (RF), and a number of small rural towns, as well as water from forest lands and agricultural fields of the water catchment area. The total solid flow of the river is 462 thousand tons with an ionic flow of 157 thousand tons [16]. In this part of the bay, fresh and salty seawaters are mixed, which leads to the continuation of flocculation processes and the formation of Fe/Mn oxides and hydroxides. In addition, the water saturates with biogenic elements, which contributes to a high degree of eutrophication of the waters of Amur Bay [17], as well as pollution with various toxic substances.

On the shore of Ussuri Bay, there is a landfill of household solid waste (HSW) in Vladivostok which was recultivated in 2012, which is a source of strong local pollution of the marine environment with heavy metals [18,19]. In addition, the water area accumulates trace elements coming from the Artemovka River flow surrounded by agricultural land, as well as from the sewage of Bolshoy Kamen, which hosts a ship repair yard.

Many scientific papers have shown that Amur Bay and Ussuri Bay are among the most polluted areas of Peter the Great Bay [20–22]. This situation was observed starting from the 1990s, which was associated with the increased development of industry [23]. Here, in 1980, the content of Zn, Cu, Pb, Hg, and Ni increased 1.5–5.0-fold as compared to background concentrations corresponding to the period before 1900 [24]. This was followed by a decline in industrial volumes since 1990 that contributed to the improvement of the environmental situation [25] and decrease of the concentrations of heavy metals in water [9,26,27]. In the period until 2012, there was a gradual self-purification of marine waters, accompanied by a 2–8-fold decrease of the content of HM in bottom sediments, except for Cu and Cd, which could be due to the reduction of the discharge of household waste into the aqueous environment [19]. The recent studies (2019–2021) showed that the contents of some elements, for example, Mn, Ni, and Pb, did not virtually change and equaled to about 340, 30, and 40 mg/kg, respectively, unlike Cu and Zn, where the content of which increased disproportionately over the years and equaled to 90 and 210 mg/kg, respectively [28]. Here, the increased content of heavy metals could be due to the fact that they enter aqueous ecosystems along with the allochthonous surface runoff as part of highly dispersed particles of suspensions, as well as a result of the situation that most of them are typomorphic elements. The effect of the monsoon climate and tropical typhoons prevailing in the warm season on the shelf zone is accompanied by a change in sedimentation, as a result of which the amount of BS carried out by rivers in both bays increases by many times. Humus substances containing chemical elements, HM in particular, accumulated by hydrobionts and plants as a result of the life cycle, affect the BS composition of water areas, which also contributes to changes in the chemical composition and migration of elements in the aqueous medium. A number of studies [29,30] show a significant excess of the contents of Fe, Ni, Si, Zn, and Pb in green and brown algae, which is, probably, due to atmospheric precipitation and secondary pollution from bottom sediments.

The basin of Lake Khanka (Xingkai) and the lake itself are characterized with a rich bioresource potential and are of great international importance as a territory preserving

the unique biodiversity of Northeast Asia, since it is a key part of the Asian migration route of birds, and, also, of considerable interest from the perspective of the economy of the Northeast of China and the Russian Far East. The lake was formed as a result of the destruction and sinking of the earth's crust. The lake area ranges from 3940 to 5010 km², reflecting fluctuations in precipitation between seasons and years. The average and maximum depths of the lake are 4.5 and 10.6 m, respectively. The relief of the lake's catchment basin is characterized by a transition from mountain ranges of medium-mountain and low-mountain relief to a zone of mounded and hummocky relief and, as a consequence, to high and low accumulative plains. In general, the basin is quite flat, especially in the northern and eastern parts, which contributes to the complex hydrology of the area. The main basin contains approximately 23 rivers flowing into the lake, 8 from China, and 15 from Russia. The hydrological regime of Lake Khanka and its capacity characteristics are determined by natural (precipitation, river runoff, evaporation from the lake's water surface) and anthropogenic (economic activity in the lake's catchment area and the transfer of runoff) factors.

According to the background hydrochemical composition, the waters of the lake and the rivers of its basin belong to the Far Eastern type, which is characterized by a small amplitude of fluctuations in the amount of dissolved salts over time and the absence of a clearly expressed relationship between flow rates (levels) and mineralization, which generally varies within 0.06–0.12 g/dm³. Unlike the lake, the mineralization of the waters of Peter the Great Bay varies in the range 28–33 g/dm³. The water of the lake and the rivers of the basin belong to the bicarbonate-calcium type. The pH value of the lake water varies in the range of 7.4–7.6 in summer and drops slightly in winter (7.0–7.2) [31].

The main problem in the state of the surface waters of the Lake Khanka basin consists in their pollution with biogenic substances. The trophic nature of water basins characterizes the content of biogenic elements, while the distribution of pollutants in the lake is uneven. The area of maximum biogenic pollution refers primarily to the area adjacent to the mouth of the Spasovka River [31].

A substantial contribution to the pollution of the basin is made by wind erosion of agricultural lands of the Chinese territory of the basin. According to Chinese experts, about 1115 km² of land undergoes wind erosion of soils on the territory of China. On the arable land, erosion reaches up to 2 mm per year, which is almost 30,000 tons per 1 km² per year. According to preliminary estimates, total soil losses in the Chinese sector reach 235×10^4 m³ per year. With this volume of soil, about 5×10^3 tons of nitrogen compounds are lost, the same amount of phosphorous compounds, and up to 4×10^4 tons of potassium compounds. As for the state of lake waters, the waters of the Little Khanka are generally more polluted by the main macro components than the waters of the main Lake Khanka [32]. The ecological situation in the Lake Khanka basin is of a primary concern. Regular discharge of poorly treated or not treated wastewater from agricultural and industrial enterprises constitutes the main anthropogenic factor that adversely affects the environmental situation. Sewage spills also often occur due to the deterioration and damage to the water supply and sanitation networks of local residential areas. As a result, pollutants enter the soil, creeks, and eventually the lake. Territories of the Lake Khanka water basin on the Russian side were actively developed for agricultural purposes over the past 10 years. The areas of cultivated land increased, so did the volumes of fertilizers and chemical crop protection products used in these areas. In this regard, the assessment of the current state of the lake's environment is an urgent task [31].

The authors of [33] stated that most HM dissolved in water (Al, Cr, Mn, Fe, Co, Ni, Cu, Zn, As, Cd, and Pb) were characterized by seasonal fluctuations in concentration, which is related to changes in hydrological and hydrochemical conditions depending on the time of year. The highest concentrations of Mn, Fe, Pb, and Zn were observed, and their average values over the entire water basin equaled 1.4, 0.4, 0.03, and 0.035 mg/L, respectively. Here, the increased contents of Mn and Fe could be related to the fact that these elements were

of the terrigenous origin, while the increased content of the rest probably indicated the influence of the discharge of household and industrial wastewaters.

Characteristic features of the lake's water consist in its high turbidity and high content of BS in it from the end of March to the end of October, while, during freezing in winter, their content drops to 5–11 mg/dm³ [31]. It was established that the content of HM in BS was inversely proportional to the BS amount [33]. For instance, in the coastal southern and southeastern parts of the lake, where the amount of BS was the lowest, the maximum Mn content was observed, which equaled to 6000 mg/kg. Another characteristic feature is a significant difference of HM between the indicators in water and BS. With a minimum content of metals in water, their values in BS exceed 10–100-fold and are equal to 32,300 mg/L for Fe, 28,000 mg/L for Al, 70 mg/L for Cu, 46 mg/L for Cr, 68 mg/L for Ni, 125 mg/L for Zn, and 41 mg/L for Pb.

Al and Fe are the main structure-forming elements in the suspension particles, which are formed as a result of the destruction and weathering of rocks, and, therefore, they enter into Lake Khanka as a terrigenous drain. As for the remaining elements, the ways of how they enter the aquatic environment and the distribution mechanisms in the BS composition are not completely clear and require additional research. Another issue is the process of studying the bottom sediments of Lake Khanka, since its peculiar bottom structure and relatively shallow depth does not allow the use of traditional oceanological equipment for core sampling.

Table 1 presents the results of the analysis of BS in the water basins of Amur Bay, Ussuri Bay, and Lake Khanka regarding the HM content. The presented data indicate the constant variability of the HM concentration, which is associated with both hydrological atmospheric changes and migration features of these elements.

Table 1. Periodic data on HM concentrations in BS of seawater and freshwater bodies of Primorsky Krai.

Water Basin	Period	Cr mg/kg	Mn mg/kg	Fe g/kg	Ni mg/kg	Cu mg/kg	Zn mg/kg	Pb mg/kg	Ref.
Peter the Great Bay (Background)	1982–2002	10.3	76	7.2	4.9	5.1	24	5.1	[34]
Ussuri Bay	2002	5–28	32–375	10–29	4–21	5–20	25–80	4–25	[34]
	2004	-	-	-	7.2	15	43	28.0	[35]
	2008	-	-	-	7.9	13	26	9.5	[35]
	2012	-	-	-	4.8	25	61.5	29.5	[19]
Amur Bay	2004	-	-	-	13.8	15	103	20.4	[21]
	2005	37	-	-	22	16	90	16.3	[29]
	2008	-	-	-	13.9	15	64	15.7	[21]
	2010	24–42	-	-	22–73	10–70	50–260	3–35	[21]
	2016	61.7	705	33.8	106.7	574	406	58.5	[36]
Khanka	2008	-	-	50.8	-	-	-	-	[37]

The objective of the present work was to establish the dependence of the HM content in the bottom sediments of seawater and freshwater basins on their chemical form, as well as the concentration in the water, and the vertical distribution in the columns of bottom sediments. To do this, the following tasks were solved: assessing of the distribution of HM both on the surface layer of bottom sediments of the water bodies and on the vertical profile taking the sedimentation rate into account; establishing the features of sedimentation processes of the water bodies; performing comparative analysis and establishing the features of horizontal and vertical distribution of HM in seawater and freshwater basins of regional and international strategic importance, and assessing the ecological and geochemical state of the studied bottom sediments.

2. Materials and Methods

2.1. Sampling

The seawater basins of Ussuri Bay and Amur Bay, which wash the shores of Vladivostok (Primorsky Krai, Russia) and are part of Peter the Great Bay (Sea of Japan), were selected as objects of the research. Lake Khanka (Xingkai) was investigated as an example of a freshwater basin. In the summer period of 2021–2022, 7 samples of bottom sediments were taken: 2 from Ussuri Bay, 2 from Amur Bay, and 3 from Lake Khanka (Xingkai), respectively. In addition, a soil sample (L-4, soil) was taken from the shore of the lake. The sampling characteristics are presented in Tables 2 and 3, respectively.

Table 2. Characteristics of sampling BS and soil.

No.	Marking	Water Basin	Latitude	Longitude	Sampling Depth, m	Core Capacity, cm
1	BS-1	Peter the Great Bay	43.16305	131.75941	11.1	27
2	BS-2		43.30395	131.79743	10.3	65
3	BS-3		43.14897	132.06444	10.2	30
4	BS-4		43.05466	131.82171	12.1	50
5	L-1	Lake Khanka (Xingkai)	44.80254	132.60453	3.5	28
6	L-2		44.90474	132.65413	3.5	24
7	L-3		44.74985	132.52311	3.6	26
8	L-4 (soil)		44.75125	132.77482	3.8	20

Table 3. Characteristics of water sampling.

No.	Marking	Water Basin	Sampling Date	Latitude	Longitude	Sampling Depth, m
1	W-1	Peter the Great Bay	June 2021	43.20835	131.81766	3–5
2	W-2		October 2022	43.08461	131.74831	
3	W-3		June 2021	43.16061	132.1024	
4	W-4		October 2022	43.08544	132.00833	
5	W-5	Lake Khanka	June 2021	44.86484	132.62309	
6	W-6		October 2022	44.75380	132.12046	

The samples were taken using a modified percussion forcer bore [38] with a sampler diameter of 110 mm. The collected cores of a thickness of 30–65 cm were delivered to the laboratory of the Institute of Chemistry of the Far Eastern Branch of the Russian Academy of Sciences (Vladivostok, Russia). After drying, the BS cores from Lake Khanka were divided into horizons with a thickness of 0.5 cm, and the cores from Amur Bay and Ussuri Bay were divided into horizons of 1.0 cm each. Each individual slice was placed in a new polypropylene beaker, weighed, and then dried in a drying cabinet at 105 °C for 8 h. In the end, the sediment was homogenized, re-weighed, and preserved in a plastic container.

The soil core was sampled using a 5 × 6 cm metal profile. The core was cut into 1 cm increments and packed in shipping bags. For further work, the obtained samples were also delivered to the laboratory, where they were sequentially weighed, dried (105 °C, 8 h), homogenized, and sealed in plastic containers for further processing.

To analyze the contents of metals in dissolved form, samples of seawater and freshwater were taken in the summer and winter of 2021–2022 (Table 3) in a volume of 50 L from a depth of 3–5 m. Under laboratory conditions, the samples were filtered from suspended matter by a blue ribbon filter and preserved by acidification to pH 3 using concentrated nitric acid.

2.2. Physical–Chemical Methods of Analysis

Determination of the concentrations of elements in water and assessment of the phase and elemental composition of the BS were carried out at the Institute of Chemistry of the Far Eastern Branch of the Russian Academy of Sciences, Vladivostok.

The phase composition of the BS was determined by means of X-ray diffraction analysis (XRD) using an Advance D8 device (Bruker) with $\text{CuK}\alpha$ radiation in the angle range $2^\circ < 2\theta < 90^\circ$ in the point-by-point scanning mode. The maximum deviation of the position of the reflexes determined by NIST SRM 1976 was less than $0.01^\circ 2\theta$. X-ray images were processed and interpreted using the Fityk and QualX software.

Elemental analysis of the BS samples was carried out using a Shimadzu EDX-800HS energy-dispersive X-ray fluorescence spectrometer by pressing a sample weight of 200 mg into a boric acid substrate and then measuring it in a vacuum. The measurement time in each area of the Ti-U, C-Cs definitions was 200 s, the collimator was 10 mm. The relative error of the method was 1–5%, depending on the element to be determined.

The concentrations of elements in freshwater and seawater samples were determined by the atomic absorption method (AAS) via the atomic absorption spectroscopy method using a SOLAARM6 bi-beam spectrometer (Thermo, Waltham, MA, USA) with a Quadline deuterium background corrector in the flame mode. The relative error of the method was 5–10%. In addition, the metal content in contact solutions was determined using an Agilent 7500C quadrupole (ICP-MS).

The contents of gamma-emitting radionuclides (^{137}Cs , ^{210}Pb) were determined at the Department of Radiochemistry of Lomonosov Moscow State University (Moscow, Russia) using an ORTEC GEM-C5060P4-B gamma spectrometer with a semiconductor detector made of ultrapure germanium (HPGe) with a beryllium window and a relative efficiency of 20%. The activity was calculated using the Spectraline software package, which allows taking into account the density and self-absorption of radionuclides by a sample. This is especially important at calculating the registration of ^{210}Pb , since it has a low gamma-line energy and a small quantum yield. The weights of the samples ranged from 1.2 to 12 g. The measurement time was at least 60,000 s. Systematic uncertainties included: sampling (3%), sample preparation (2%), and measurement (2%), and in total, they did not exceed 8%.

A constant flow model was used to determine the age of bottom sediments and sedimentation rate based on ^{210}Pb content [39]:

$$t = \frac{1}{\lambda} \ln \ln \frac{A(\infty)}{A(x)} \quad (1)$$

where t is the age of a sediment, years; $A(\infty)$ is the activity of the surface horizon calculated based on the smoothed function of the distribution of reserves by depth, Bq/m^2 ; $A(x)$ is the specific activity of a horizon, Bq/m^2 ; λ is the radioactive decay constant ^{210}Pb .

To determine the age of individual layers of bottom sediments using technogenic ^{137}Cs , a peak was identified on the plot of its vertical distribution, which corresponds to the maximum of global precipitation in 1963 (the main nuclear weapons tests in the Northern Hemisphere) [40].

The degree of contamination of heavy metals in each sample was estimated using the concentration coefficient (C_s) according to [41], which was determined and calculated as follows:

$$K_c = \frac{C_i}{C_b} \quad (2)$$

where C is the concentration of the detected substance in the test (i) and background (b) samples.

The HM geoaccumulation index was calculated by comparing the concentration of metal in the studied samples with their base level in the Earth's crust [42] according to the following formula:

$$I_{geo} = \log_2 \frac{C_{bs}(M)}{1.5 \times C_c(M)} \quad (3)$$

where $C_c(M)$ is the base concentration of metal in the Earth's crust, mg/kg [43]. The multiplying coefficient 1.5 is a coefficient to minimize changes that may occur with the base concentration of metal due to geological changes in bottom sediments. There are seven classes of the geoaccumulation index [44]: $I_{geo} \leq 0$ —unpolluted; $0 < I_{geo} < 1$ —unpolluted to moderately polluted; $1 < I_{geo} < 2$ —moderately polluted; $2 < I_{geo} < 3$ —moderately to strongly polluted; $3 < I_{geo} < 4$ —strongly polluted; $4 < I_{geo} < 5$ —strongly polluted to extremely polluted; $4 < I_{geo}$ —extremely polluted.

The migration ability of HM from water to bottom sediments was estimated using the distribution coefficient [45]:

$$I_g K_d = \frac{C_{bs}(M)}{C_w(M)} \quad (4)$$

where $I_g K_d$ is the distribution coefficient; $C_{bs}(M)$ is the metal content in bottom sediments, mg/kg; $C_w(M)$ is the metal content in water, mg/L.

The HM content in water was estimated against the background of maximum permissible concentrations (MPC) for natural water basins in the Russian Federation [46]. According to the established values, the contents of HM in water basins should not exceed the following values: Cr ≤ 70 µg/L, Mn ≤ 10 µg/L, Fe ≤ 100 µg/L, Ni ≤ 20 µg/L, Cu ≤ 100 µg/L, Zn ≤ 100 µg/L, and Pb ≤ 10 µg/L.

The calculation of K_c and I_{geo} values was carried out using Microsoft Excel and Jamovi version 2.3.28. using the above equations. The SigmaPlot software version 13.0 was used to represent the obtained data in a graphical form. For all calculations, the confidence interval was at least 0.98.

3. Results and Discussion

The cores collected in Peter the Great Bay are presented in the form of a mixture of sandy and chemogenic (clay) deposits, while the latter are predominant in the waters of Amur Bay (Figure 1), which is reflected in the oiliness of the samples and a pungent smell of hydrogen sulfide. Visually, the composition of BS can be divided into several horizons. In particular, the BS-1 and BS-2 samples (Figure 1a,b) are characterized by an increased content of sapropel, which begins with a dense compressed layer (0–7 cm), with a partial admixture due to the content of sand particles (7–17 cm), and the transition to clay-like sediments of light (17–22 cm) and heavy (22–40 cm) types. The BS-3 sample (Figure 1c) was taken from Ussuri Bay and had a characteristic terrigenous origin, which is reflected in the predominance of fragmental rocks (0–10 cm) with a transition to heavy clay-like sediments (10–30 cm). The BS-4 sample (Figure 1d) has a composition similar to the samples from Amur Bay except for the upper layer (0–5 cm), the composition of which is represented by calcareous clay silts due to the high content of bivalve mollusk remains. Annealing of various horizons of the BS profile to 650 °C was accompanied by a decrease of the sample mass by 3–7% (Ussuri Bay) and 9–13% (Amur Bay). A decrease of the sapropel content in BS-3 was accompanied by an increase in the density of horizons by 1.5–2 times, unlike other BS that had a value of about 1.2–1.5 g/cm³ (Figure 1g). Here, the sediment density is rather uniform throughout the profile, which indicates a uniform sedimentation and the absence of abnormal influence of natural or anthropogenic factors on this process.

Figure 2 shows the BS cores from Lake Khanka (Xingkai), as well as soils collected close to the coastline (Figure 2d). Unlike the seawater BS, all samples from freshwater basins have a terrigenous origin and are presented in the form of compressed sand and thin clays, the layers of which are probably formed due to grain flows. All the BS samples are characterized by separation into layers of light brown sand (0–2 cm), dark gray clay (2–13 cm), dark clay (13–14 cm), coarse-grained sand with foreign inclusions (14–16 cm), and clay with iron oxide inclusions (16–25 cm). The L-2 sample (Figure 2b) is characterized by an increased content of clays. It was found that the vertical sediment density increased with the transition to deeper horizons (Figure 2e–g), which indicated an increase of the rate of sedimentation in recent decades due to the rise in water levels during increased precipitation, accompanied by the expansion of the wetland area adjacent to the lake. The

proportion of the organic component established during the annealing process was 2–3% and 4% for the BS and soil, respectively. The collected sample belongs to the meadow texture-contrast soil. This type of soil is characterized by a powerful layer of organogenic horizon (up to 18 cm) of dark gray color of a strong fine-grained structure, abundantly permeated with grass roots and soil animal tracks. The boundary to the underlying horizon has a flowing shape. The next horizon demonstrates signs of gleization, in our case, it is slightly carbonaceous and of brownish-ochre color (Figure 2d,h). The soil is rich in nutrients such as ozone and phosphorus.

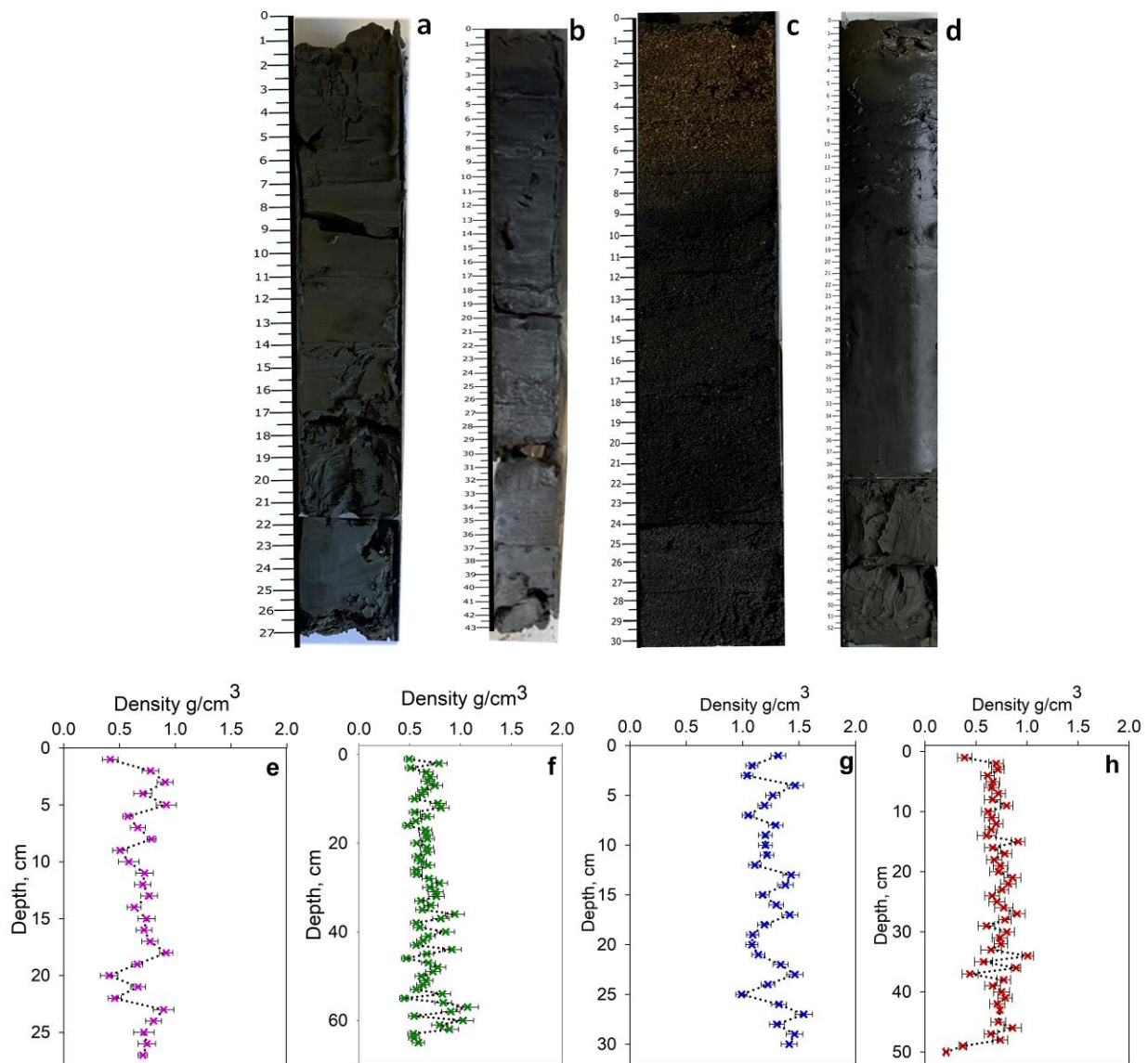


Figure 1. Appearance and distribution of the BS core density in Peter the Great Bay: (a,e) BS-1; (b,f) BS-2; (c,g) BS-3; (d,h) BS-4.

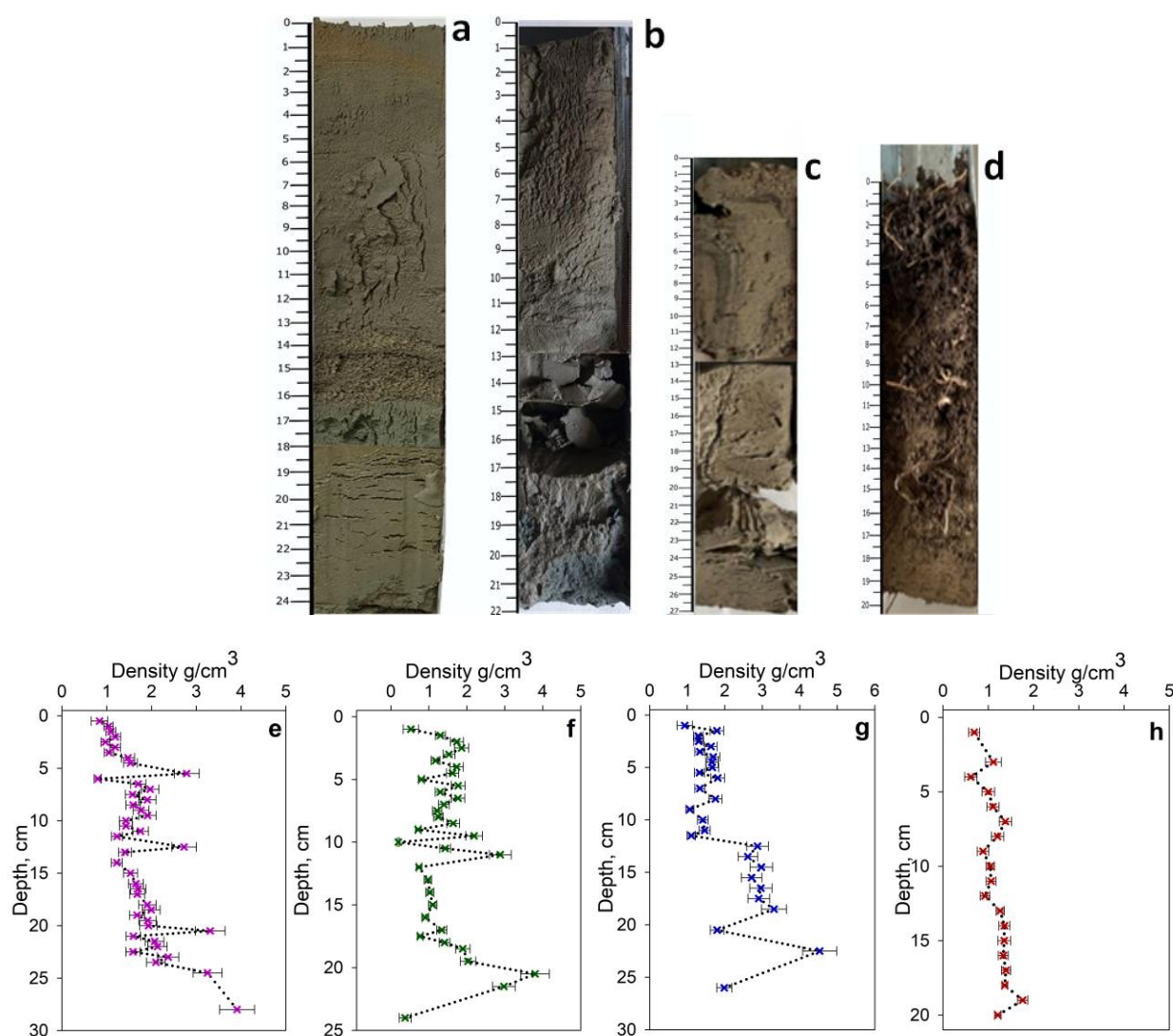


Figure 2. Appearance and density distribution of the cores from Lake Khanka (Xingkai): (a,e) L-1; (b,f) L-2; (c,g) L-3; (d,h) L-4 (soil).

3.1. Assessment of the Pollution Level

To establish the ecological state and the regional geochemical background, the average HM content in the upper layer of the sea (Table 4) and freshwater BS (Table 5) was calculated. The obtained values of the HM content in the upper 5 cm of an undisturbed BS profile were used for the calculation. The average values of concentration of metals in the sea sediments in the environment unaffected by economic activity at the station on Reyneke Island (Peter the Great Bay, Sea of Japan (Figures 1–3) for the period 1982–2002 [34,47] were used as background levels of the concentration of metals.

Table 4. The values of the HM content on the surface of Peter the Great Bay, dry matter.

Marking	Indicator	Cr, mg/kg	Mn, mg/kg	Fe, g/kg	Ni, mg/kg	Cu, mg/kg	Zn, mg/kg	Pb, mg/kg
BS-1	Aver	270 ± 70	730 ± 20	105 ± 3	70 ± 15	1100 ± 70	455 ± 20	90 ± 25
	Max	375 ± 45	750 ± 160	109 ± 4	95 ± 25	2890 ± 55	845 ± 85	130 ± 25
	Min	200 ± 45	670 ± 160	99 ± 4	45 ± 25	870 ± 55	360 ± 85	50 ± 25
	K _c	6.6	2.1	30.1	1.6	3.8	4.5	2.6
	I _{geo}	1.13	−1.04	0.59	−0.32	0.59	0.83	12.19

Table 4. Cont.

Marking	Indicator	Cr, mg/kg	Mn, mg/kg	Fe, g/kg	Ni, mg/kg	Cu, mg/kg	Zn, mg/kg	Pb, mg/kg
BS-2	Aver	250 ± 40	750 ± 40	112 ± 7	80 ± 20	200 ± 15	325 ± 10	135 ± 20
	Max	285 ± 45	820 ± 160	107 ± 4	125 ± 25	290 ± 55	340 ± 85	185 ± 25
	Min	220 ± 45	675 ± 160	116 ± 4	55 ± 25	90 ± 55	320 ± 85	80 ± 25
	K _c	6.1	2.1	32.1	1.7	7.2	3.2	3.9
	I _{geo}	1.01	−1.00	0.69	−0.17	1.51	0.35	12.77
BS-3	Aver	300 ± 60	700 ± 200	94 ± 10	95 ± 25	1530 ± 80	2225 ± 150	1300 ± 100
	Max	650 ± 45	1150 ± 160	123 ± 4	120 ± 25	2890 ± 55	5070 ± 85	3093 ± 25
	Min	120 ± 45	405 ± 160	65 ± 4	45 ± 25	870 ± 55	1180 ± 85	430 ± 25
	K _c	7.3	2.0	26.9	2.1	54.6	22.2	37.2
	I _{geo}	1.26	−1.10	0.43	0.09	4.44	3.13	16.03
BS-4	Aver	180 ± 35	725 ± 50	100 ± 5	60 ± 15	420 ± 50	400 ± 35	140 ± 25
	Max	220 ± 45	800 ± 160	106 ± 4	90 ± 25	455 ± 55	490 ± 85	200 ± 25
	Min	125 ± 45	660 ± 160	96 ± 4	45 ± 25	370 ± 55	370 ± 85	95 ± 25
	K _c	4.4	2.1	28.5	1.3	15.1	4.0	4.0
	I _{geo}	0.53	−1.05	0.52	−0.57	2.58	0.65	12.82
BACKGROUND *		41	150/350	1.5/3.5	15/45	8/28	30/100	20/35
Clarke **		83	1000	46.5	58	47	170	0.013

Notes: BACKGROUND *—background values of HM content in Peter the Great Bay: Cr [34], other HM [47] (sands/aleuropelites); Clarke **—the content of elements in the lithosphere, according to Vinogradov A.P. [43].

Table 5. The values of the HM content on the surface of Lake Khanka (Xingkai), dry matter.

Marking	Indicator	Cr, mg/kg	Mn, mg/kg	Fe, g/kg	Ni, mg/kg	Cu, mg/kg	Zn, mg/kg	Pb, mg/kg
L-1	Aver	125 ± 25	1210 ± 150	48 ± 5	40 ± 10	255 ± 30	180 ± 30	0
	Max	145 ± 25	1340 ± 165	55 ± 4	60 ± 15	290 ± 55	230 ± 35	0
	Min	105 ± 25	935 ± 165	45 ± 4	50 ± 15	145 ± 55	135 ± 35	0
	K _c **	1.5	1.2	1.0	0.7	5.4	1.1	0.0
	I _{geo}	0.02	−0.31	−0.54	−1.16	1.86	−0.50	−1.16
L-2	Aver	125 ± 15	1535 ± 80	54 ± 2	55 ± 10	285 ± 25	200 ± 30	90 ± 5
	Max	135 ± 25	1655 ± 165	57 ± 4	60 ± 15	325 ± 55	245 ± 35	100 ± 15
	Min	120 ± 25	1380 ± 165	59 ± 4	50 ± 15	245 ± 55	135 ± 35	80 ± 15
	K _c **	1.5	1.5	1.2	1.0	6.0	1.2	6784.6
	I _{geo}	0.03	0.03	−0.37	−0.65	2.01	−0.37	12.14
L-3	Aver	175 ± 10	3460 ± 900	79 ± 7	0	335 ± 15	530 ± 20	85 ± 5
	Max	180 ± 25	4575 ± 165	92 ± 4	0	365 ± 55	795 ± 35	85 ± 15
	Min	165 ± 25	1935 ± 165	67 ± 4	0	305 ± 55	335 ± 35	85 ± 15
	K _c **	2.1	3.5	1.7	0.0	7.1	3.1	6625.4
	I _{geo}	0.50	1.21	0.18	< 0	2.25	1.05	12.11

Table 5. Cont.

Marking	Indicator	Cr, mg/kg	Mn, mg/kg	Fe, g/kg	Ni, mg/kg	Cu, mg/kg	Zn, mg/kg	Pb, mg/kg
L-4 (soil)	Aver	110 ± 10	7400 ± 1000	83 ± 5	80 ± 20	395 ± 40	375 ± 80	120 ± 30
	Max	130 ± 25	9475 ± 165	92 ± 4	95 ± 15	510 ± 55	510 ± 35	165 ± 15
	Min	80 ± 25	6110 ± 165	76 ± 4	60 ± 15	365 ± 55	260 ± 35	80 ± 15
	K _c **	1.3	7.4	1.8	1.3	8.4	2.2	9225.8
	I _{geo}	−0.19	2.30	0.25	−0.16	2.49	0.55	12.58
Clarke *		83	1000	46.5	58	47	170	0.013

Notes: Clarke * is the content of elements in the lithosphere, according to Vinogradov A.P. [4]. K_c ** is the ratio of C(Mi) to C(Mi)_{clark}.

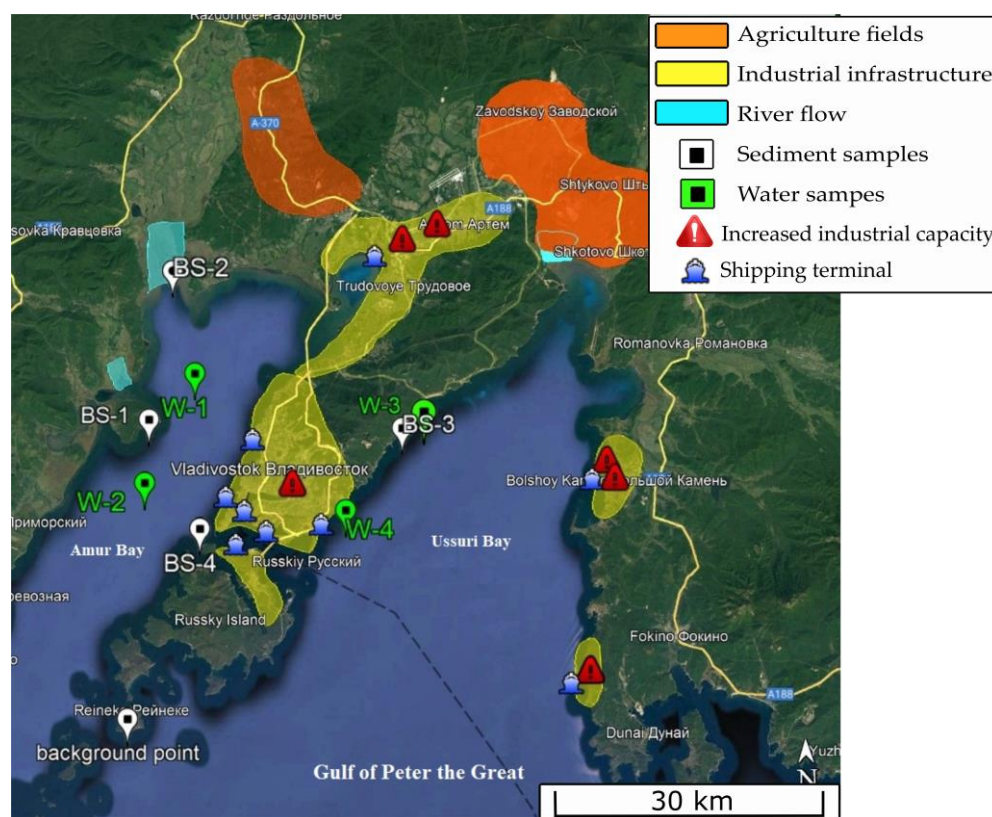


Figure 3. Map of the estimated areas of the HM polluting sources in Peter the Great Bay.

It was established that the concentration values of all HMs in the BS of Peter the Great Bay exceeded the background [34,47] and lithosphere [43] values by two or more times (Table 3). The average values of the concentration of elements decrease in the following row: Fe > Cu > Cr > Zn ≥ Pb > Mn > Ni. Figure 3 shows a map of the estimated pollution sources established according to the calculated concentrations of HM. The greatest excess of concentration was recorded for Fe across the entire water body of the bay, the source of which is probably organic and inorganic suspensions in the composition of river drains (green area, Figure 3: Artemovka river, Razdolnaya river, Amba river). When exposed to a medium with pH > 6 and an elevated salt background, iron is transferred into the corresponding hydroxide forms $[\text{Fe}(\text{OH})]^{2+}$, $[\text{Fe}(\text{OH})_2]^+$, $[\text{Fe}(\text{OH})_3]^0$. In the above water basins, this process is reflected by the increased turbidity of water in coastal areas, which is additionally amplified by wind stirring. Only a small part of particularly fine suspensions reaches the open part of the sea, while most of the solids and solutes are retained in the barrier zone. Thus, a decrease of the Fe content in the BS samples from Amur Bay from the estuary part (Figure 3 BS-1) to the bay mouth (Figure 3 BS-2) indicates a decrease in the

influence of terrigenous runoff. This fact is also reflected in a decrease of the Mn content in these samples, the source of which, like Fe, is a terrigenous runoff. In comparison with the background values, there are excess concentrations of Cu, Zn, and Pb by 55, 22, and 37 times, respectively, in Ussuri Bay. The excess content of these HM may be due to the sewage discharge from the city of Vladivostok, a number of large enterprises and factories located on the shore of the water area (Figure 3, yellow areas), and extensive agricultural land (Figure 3, orange areas). The following should be taken into account, particularly, a landfill of household waste located in the suburbs of Vladivostok and preserved in 2012 [11,12], and the BS-3 sampling points, capable of supporting the flow of HM entering seawater for many years with subsequent accumulation in BS. The 2–4-fold increased HM content in the BS-1 and BS-2 samples could be due to atmospheric precipitation, seasonal variability, and gradual self-cleaning of the bay, which has been observed over the past 20 years after the decline of industrial production [26]. Despite the fact that the water area where the BS-4 sample was taken was more closed and had no river drains, there was an increased content of HM in the BS, which could be determined by both the absence of internal flow and corrosion of military shipwrecks.

Bottom sediments of Lake Khanka were not studied before, since it was impossible to perform sampling using standard oceanological equipment due to the shallow depth of the water body, the constant variability of the bottom, and specific atmospheric and water weather conditions. In this regard, the established values of the HM content in the BS were estimated against the background of the Clarke number of the lithosphere [43]. As can be seen from the data presented in Table 3, the concentration values of all HMs exceed the limit values of the lithosphere, which indicates anthropogenic impact. The average concentrations of elements decrease in the following row: $Pb > Cu > Mn > Fe > Cr > Zn > Ni$ for the lake sediments, and $Pb > Cu > Mn > Fe > Zn > Cr \geq Ni$ for the coastal soil (Table 5). A significant excess of Pb in the surface layer was earlier recorded in 2018 [48]; however, the concentration values presented were 2–3-fold less than the present ones and amounted to about 10–50 mg/g. The source of pollution in this area can only be possible river tributaries that have connecting channels with lead smelting and recycling enterprises, but there is no published information about this. Here, the values obtained in the soil from the coast can serve as a basis for establishing other sources of pollution. The highest values of Mn, Fe, and Cu were established for the L-3 sample, which is associated with terrigenous flow and, probably, with abnormally rich deposits of tin ores (Figure 4 red region) [49], the main minerals of which are cassiterite (SnO_2) and stannine (tin pyrite, Cu_2FeSnS_4) containing up to 13% Cu and 28% Pb. Zn and Pb can also be present in the form of impurity metals. The Zn content in the BS is almost two times higher than the value obtained for the soil (L-4), which may be due to atmospheric precipitation during the transfer of dust particles from a zinc ore mining site (Figure 4 purple area). In addition, in the east of Primorsky Krai, one of the largest deposits of lead-zinc ores in Russia is located, which can also have an anthropogenic impact and contribute to an increase in background concentrations of Pb and Zn in soil and water bodies by means of weathering and transfer of dust particles with subsequent accumulation in the BS.

According to the calculated values of the K_c concentration coefficient (Tables 4 and 5) and the geoaccumulation index I_{geo} (Figure 5), BS of Peter the Great Bay in relation to Cr, Mn, Fe, and Ni belong to the class of unpolluted and are depleted by these elements, with the exception of iron. In Figure 5, dotted lines indicate the boundaries of the division of classes of the geoaccumulation index [44]. Despite the depletion of the BS in Cu and Zn, their class varies from unpolluted to strongly polluted, depending on the water area of the probe, which is probably closely related to the diversion of urban spillway plants. At the same time, in relation to Pb, BS of both the sea area (Figure 5a) and Lake Khanka (Figure 5b) exhibits strong pollution with directly proportional enrichment of sediments. A distinctive feature of freshwater sediments is the wide area of Mn distribution, which allows classifying these BS from unpolluted to strongly polluted. There is also a moderately strong pollution of sediments by Cu.

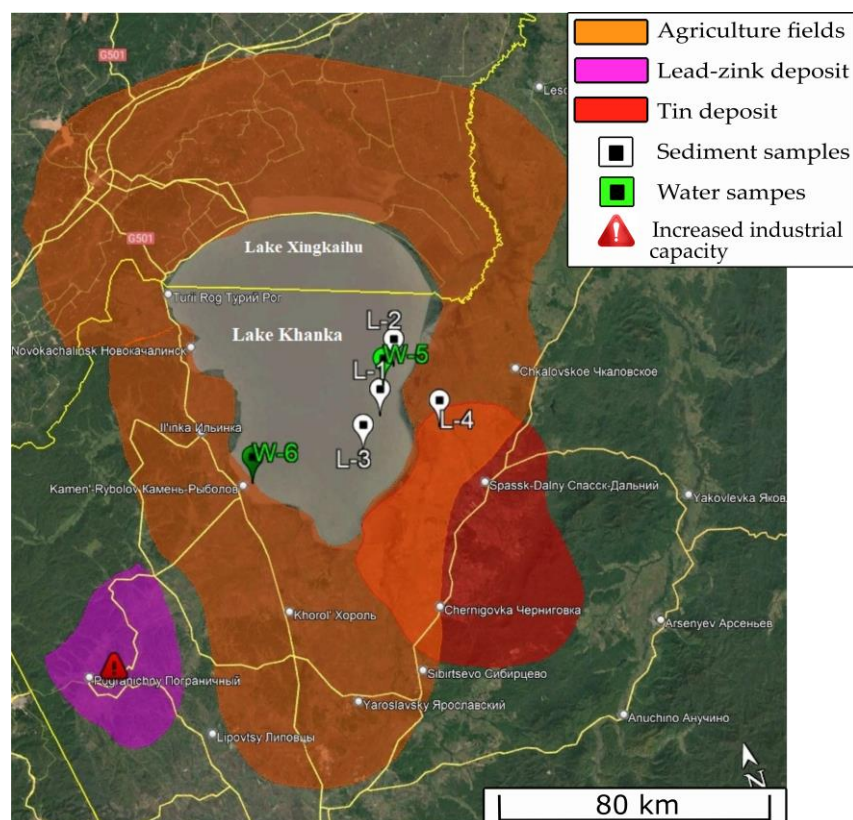


Figure 4. Map of the estimated areas of HM sources polluting Lake Khanka (Xingkai).

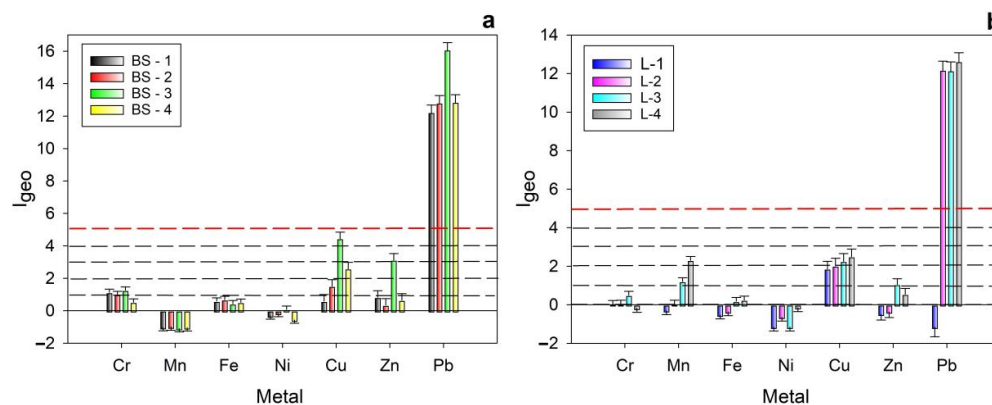


Figure 5. Dependence of the geoaccumulation index on the type of metal: (a) Peter the Great Bay; (b) Lake Khanka.

3.2. Assessment of HM Content in the Core Profile

If we neglect the process of desorption of HM from the BS back into the aqueous medium, then, the sediments can be considered as the final stage of migration of pollutants. In this case, the influence of the surrounding anthropogenic and natural factors on the process of migration, deposition, and concentration of HM can be traced by analyzing the vertical profile of the BS.

The sedimentation rate in the BS samples was estimated by measuring the activity of factory-made radionuclides ^{137}Cs and $^{210}\text{Pb}_{\text{ex}}$ by the core depth (the maximum activity corresponds to the time of the most intensive nuclear weapons tests in 1963). In earlier studies, it was found that the sedimentation rate in the northern part of Amur Bay was equal to 7.2 mm/year in 1996 [50] and 3.6–5.2 mm/year in 2015 [51]. We found that, for the central part of Amur Bay, the calculated values are 1.6 mm/year [52]. For Ussuri Bay, the sedi-

mentation rate decreased 2–3-fold compared to Amur Bay and amounted to 0.45 mm/year. This fact directly depends on the number and volume of freshwater reservoirs flowing into the water basin, which are an order of magnitude smaller in Ussuri Bay.

Figure 6 shows the dependencies of the HM concentration in the core profile, where the greatest changes were observed, from the depth of the underlying layer to in the waters of Ussuri Bay and Amur Bay. It was established that the values of Fe and Mn concentrations in Amur Bay's profile (Figure 6, BS-1/BS-2) did not undergo changes up to a depth of 50 cm (for point BS-2), which approximately corresponds to 300 years, while the maximum concentration reaches the values of 760 mg/kg (Figure 6b,i) and 120 mg/kg (Figure 6c,j), respectively. This fact indicates that, despite the seasonal change in the amount of precipitation, the terrigenous flow of these metals does not change and is in equilibrium. Additionally, it can be indirectly concluded that the mineral or organic phase of metals does not undergo significant changes over time, otherwise there would be a process of de-manganation and de-ironing accompanied by a change in the concentration of HM in the BS profile and water, as a result of changes in the physical–chemical properties of the aqueous medium (pH, concentration of free carbon dioxide, dissolved oxygen, redox potential, sulfides, organic substances, hardness, total mineralization, dissolved gases [53]).

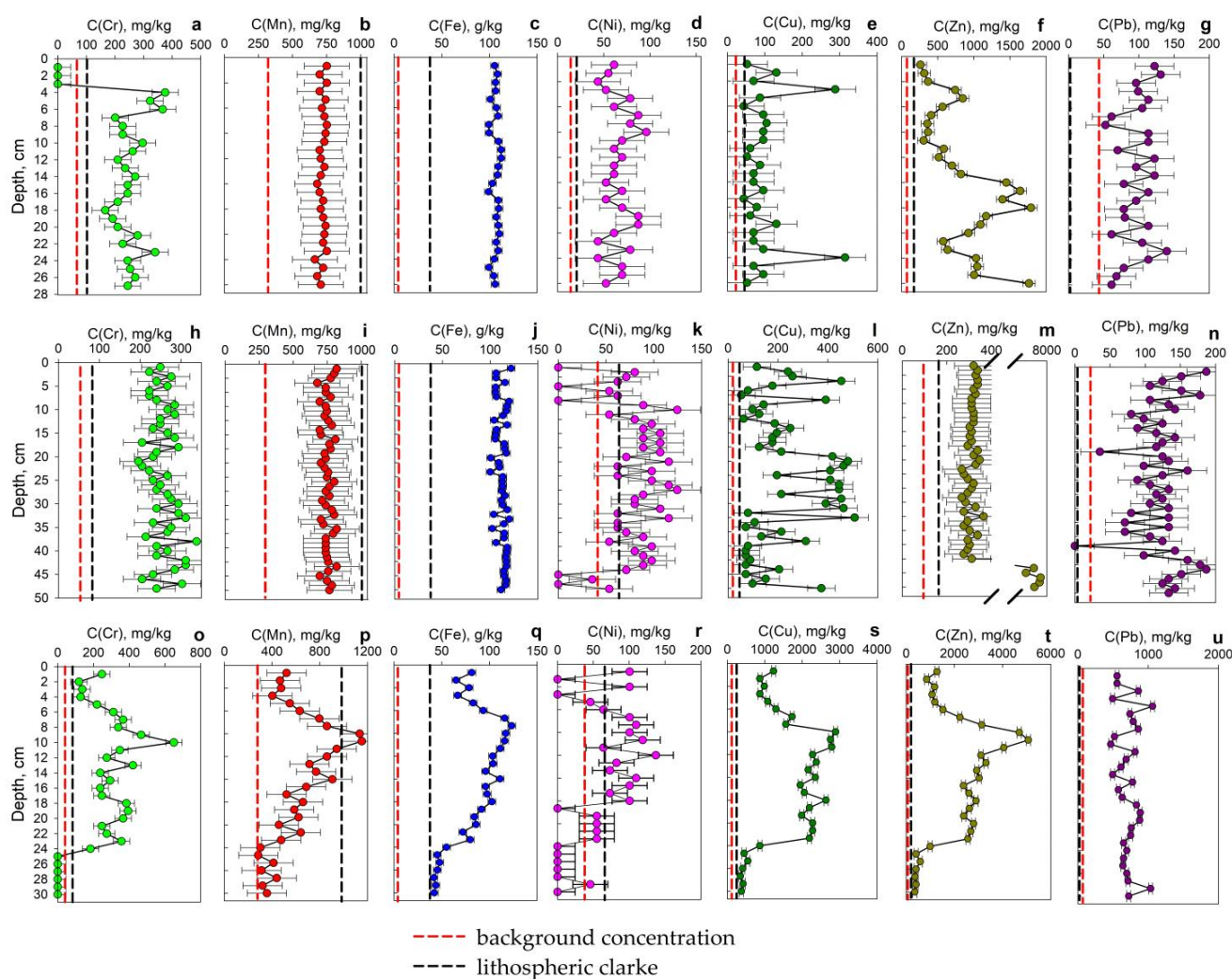


Figure 6. Profile distribution of HM in the BS cores from Peter the Great Bay: (a–g) BS-1; (h–n) BS-2; (o–u) BS-3.

In Ussuri Bay's profiles (Figure 6, BS-3), during the transition from 22 cm to 10 cm, an increase of the concentration of all the studied HM by two to three times is observed,

which could be related to the period of active development of the territories and local industry. The subsequent slowdown in the industrial development rate since the 1990s could contribute to a decrease of the level of environmental impact, which is reflected in a consistent decrease of the concentration of HM in the upper 10 cm layer of the BS [17,27].

It was found that, during the transition from the estuary (coastal) zone of the river flow of the Razdolnaya River (Figure 3, BS-2) to the central zone (closer to the outlet to the ocean, Figure 3, BS-1), the concentration of biogenic metals (Ni, Zn, Pb, Cu) in the whole profile decreased 2–4-fold (Figure 6, BS-1, BS-2), probably, due to the formation of their hydroxides and carbonates ($[\text{Ni}(\text{CO}_3)]^0$, $[\text{Ni}(\text{OH})]^+$, $[\text{Ni}(\text{OH})_2]^0$, $[\text{Zn}(\text{OH})]^+$, $[\text{Pb}(\text{CO}_3)]^0$, $[\text{Cu}(\text{CO}_3)]^0$, $[\text{Cu}(\text{OH})_2]^0$) in the area of mixing of freshwater and seawater followed by sorption on suspensions that prevent the distribution of HM over long distances as a result of the BS formation. The highest concentrations of these metals were recorded at the profile level of 36–48 cm for the near-mouth core (BS-2) and 24 cm for the central part of the bay (BS-1), which is approximately in the same time ranges. Here, the difference in the depth of the layer is compensated by the sedimentation rate, which in the BS-1 sample is approximately 1.5–2 times less than in BS-2.

Figure 7 shows the dependence of the HM concentration on the depth of the underlying layer of the BS in the water basin of Lake Khanka (sample L-2) and the profile of the coastal soil (−4). The distribution and concentration of HM in the samples L-1 and L-3 have a comparable shape and values and, therefore, were not considered in detail. It was established that the sedimentation rate in the core sampling area was about 0.43–0.50 mm/year [52].

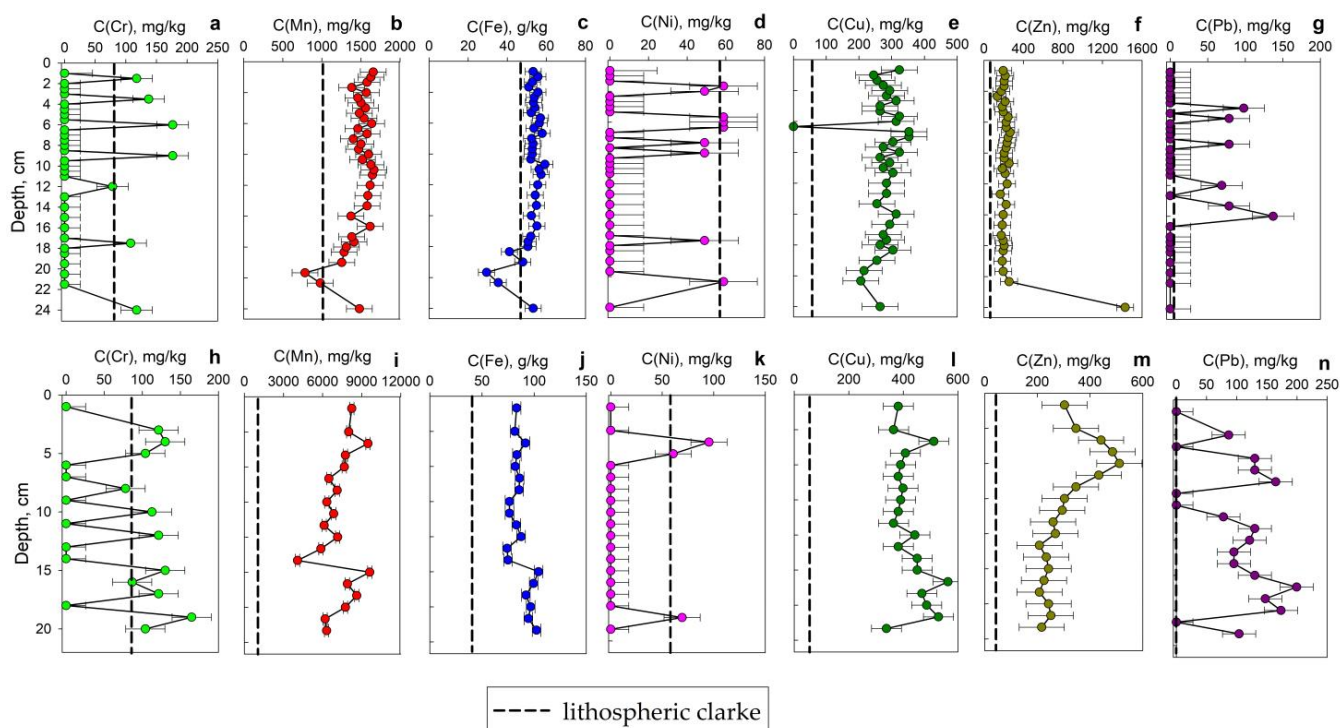


Figure 7. Profile distribution of HM in the BS cores from Lake Khanka (a–g) and the coastal soils (h–n).

Chaotic fluctuations of concentrations of Cr and Pb are observed in the BS: from 0 to 180 mg/kg (Figure 7a,g), which is also reflected in the soil profile (Figure 7h,n) with the addition of Ni (Figure 6k). The highest concentrations were recorded for Fe and Mn, which are evenly distributed over both profiles. Minor deviations are probably related to the geochemical position of certain soils in the core profile. Here, the increased Mn content is determined by the constant allochthonous runoff and the fact that it is a typomorphic element. High content of Fe in the entire profile indicates the predominant presence of a

fine grain fraction, as well as the intensive sedimentation of the suspended matter during the entire time. The same trend is typical for Amur Bay.

Comparable values of Cr and Zn concentrations in the BS and soil profile indicate an increased content of elements in atmospheric precipitation and natural runoff.

In general, the concentration values of Mn, Fe, Cr, and Pb in the soil profile exceed 2–6-fold the values obtained for the BS, which contributes to the accumulation of HM in them, at intensive release from sub-positions. This type of HM migration is characteristic of transluvial and subordinate landscapes, accompanied by the removal of HM from the soil profile. Metals migrate both in dissolved form with ground runoff and mechanically, moving to the final links of landscapes: swamps, lakes, and sea bays [54]. It is reasonable to suggest that the flow of lead into the lake began about 100 years ago and that it was associated with anthropogenic impact. The same assumption can be made about Ni. A peak of Zn content was detected in the soil profile at a depth of 6–7 cm. This was probably the result of the same anthropogenic influence, but more local, which did not affect the flow of Zn into the bottom sediments of the lake.

3.3. Phase Composition of the BS

To establish regularities of the horizontal and vertical distribution of HM in the pre-studied waters, the phase composition of these sediments was studied. Figure 8 shows X-ray images reflecting the phase composition of the BS collected in Amur Bay (BS-1, BS-2) and Ussuri Bay (BS-3). The X-ray patterns are provided only for the upper centimeter layer, since the qualitative analysis of the phase composition of subsequent horizons is comparable to horizon No. 1.

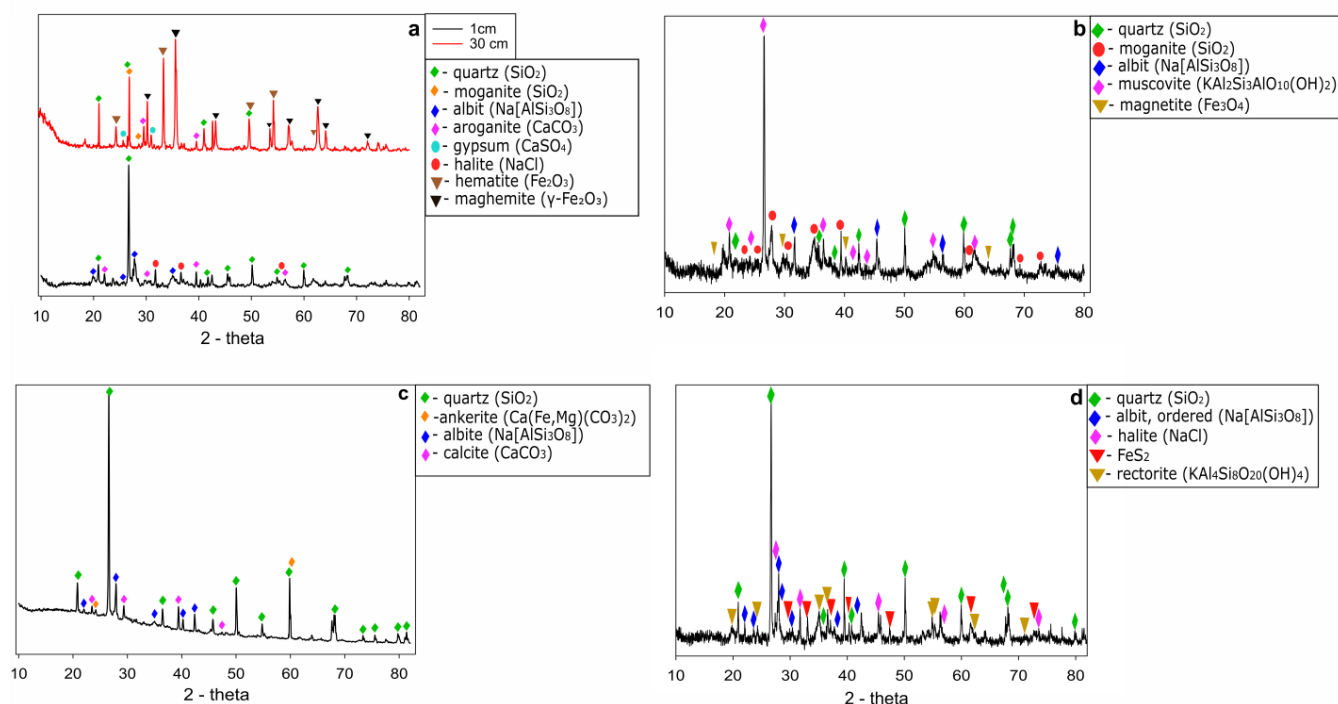


Figure 8. X-ray patterns of the BS from Peter the Great Bay: (a) BS-1; (b) BS-2; (c) BS-3; (d) BS-4.

A common feature of all the X-ray patterns consists in clearly expressed reflexes corresponding to different phases of silicon oxide (quartz, chalcedony, moganite). The source of silicic-oxygen minerals, the total content of which in the samples is 30–50%, are both coastal sand rocks and a river stream containing BB. It is worth mentioning that the presence of silicates with a developed surface morphology can be accompanied by active adsorption processes and concentration of heavy metals present in the composition of the soil, from freshwater and seawater when entering the liquid phase. However, additional studies are

required to assess the qualitative and quantitative characteristics of this transfer. A significant part of the sediments is also represented by minerals such as albite ($\text{Na}[\text{AlSi}_3\text{O}_8]$) with an admixture of calcium, calcite (CaCO_3), and ankerite ($\text{Ca}(\text{Fe,Mg})(\text{CO}_3)_2$), which could be related to the presence of bicarbonate and contribute to the accumulation of iron. Albite is the most common pore-forming mineral of magmatic origin belonging to the class of aluminosilicates, its source can include underwater and terrestrial volcanoes of the Far Eastern coast, and the waters of the Sea of Japan, in particular. The phase of calcium carbonate, which is probably related to aragonite, formed as a result of the destruction of mollusk shells and is a biogenic accumulator of HM. As the depth of the incision increases, a directly proportional increase in the intensity of the halos corresponding to the ankerite is observed, which also affects the increase in the Fe content in the studied sections of the BS-3 sample. In addition, there are reflexes corresponding to rock salt and halite with cubic syngony, the presence of which is associated with the sample preparation process that results in crystallization of NaCl contained in seawater.

A significant difference in the phase composition is observed in the samples BS-1 and BS-2 (Figure 8a,b) at a profile depth corresponding to the range of 17–50 cm, where the predominant phases were established for such relic minerals as hematite and maghemite, least of all quartz and moganite. At a profile depth of 45 cm, the phase of iron sulfide (FeS_2) was also identified; its formation can be associated with redox processes of decomposition of organic residues of biota and metal structures undergoing corrosion. The predominance of iron oxide phases coincides with the results of the elemental analysis shown in Figure 6, and, at the same time, an increase of the values of other HM is also observed, which could be related to increased sorption characteristics of hematite and maghemite [55]. In this case, maghemite and hematite can interfere with the processes of diffusion of HM back into the water.

In addition to calcium carbonate, the samples from Amur Bay also contain a phase of calcium sulfate (gypsum) of biogenic origin. The initial samples of BS contained the remains of shells of bivalve mollusks of various species.

Figure 9 shows X-ray patterns reflecting the phase composition of Lake Khanka BS (L-1, L-2, L-3). The presented patterns are provided only for the upper centimeter layer, since the qualitative analysis of the phase composition of subsequent horizons is comparable to horizon No. 1.

The phase composition of all the samples is represented mainly by quartz as part of the sand. Just like in the seawater BS, a group of widespread aluminosilicates, feldspars of igneous origin, albite ($\text{Na}[\text{AlSi}_3\text{O}_8]$), and anorthite ($\text{Ca}[\text{Al}_2\text{Si}_2\text{O}_8]$) with high contents of K and Ca impurities were identified. With an increase in the depth of the section, the intensity of the corresponding reflexes decreases, which is probably the result of changes in natural conditions and cataclysms (floods, wind, earthquakes, etc.) having a major role in the process of transferring and concentrating components. The presence of a large variety of freshwater bivalves and other mollusks in the water body, as well as an increased content of carbonates leads to the formation of calcium carbonate polymorphs, calcite, and aragonite. Iron was identified in the phase composition of ankerite ($\text{Ca}(\text{Fe,Mg})\text{CO}_3$), as well as an uncharacteristic phase for this region, ferrisanidine ($\text{KNa}[\text{FeSi}_3\text{O}_8]$) with possible admixtures of Al, Ti, Mg, and Na. Its formation was probably caused by the water migration of factory-made iron involved in subsequent biogenic processes. Here, the percentage of iron-forming phases does not change with depth. An additional contribution of iron to the phase composition to the lake could be made by intraplate volcanites and intrusions of mixed magmatic series lying at a distance of 20–80 km from the southern and western shores of the water body [56]. The composition of these rocks includes minerals such as basalt, andesites, dacites, rhyolites, and their tuff-sedimentary rocks containing from 1 to 10% of Fe_xO_y , depending on the type of mineral.

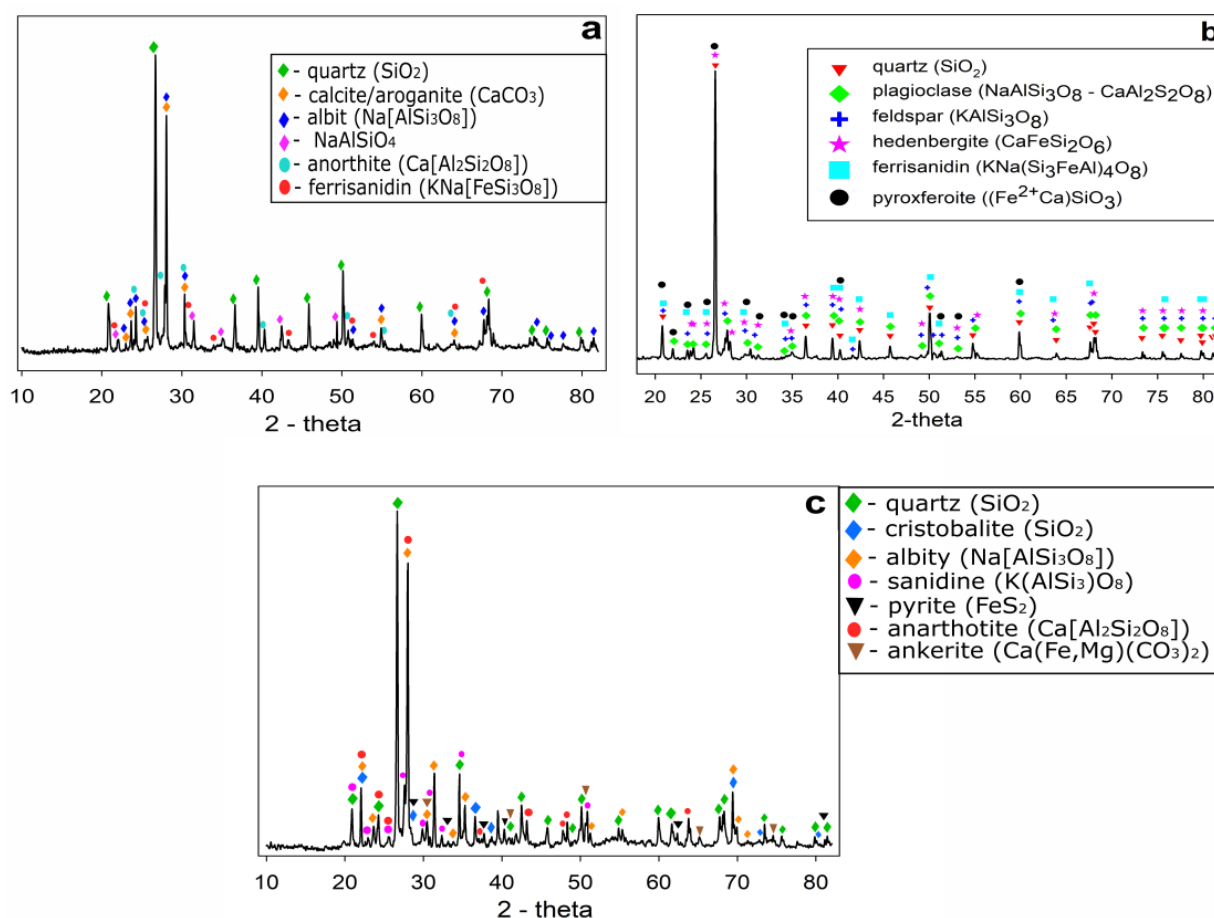


Figure 9. X-ray patterns of Lake Khanka BS: (a) L-1; (b) L-2; (c) L-3.

3.4. HM in the Liquid Phase

Since the migration of heavy metals in water bodies directly depends on the features and mechanisms of the two-way transition of elements in the water–bottom sediment system, the contents of the base (Table 6) and heavy metals (Table 7) in the investigated aqueous objects were studied. The values of the content of base metals (Table 7) in the seawater and freshwater basins correlates to regional data for many years [19–21,25,28,57]. On the contrary, the values of the HM content (Table 7) demonstrate an excess compared to previous years [20,21]. In comparison with the maximum permissible concentrations of the Russian Federation (MPC), the World Health Organization (WHO), the US Environmental Protection Agency (US EPA), and environmental protection agencies of China and Japan, Peter the Great Bay has an excess of Mn—2-fold, Fe—2-fold, and Zn—3-fold. The ratio of the HM concentration to MPC in Lake Khanka is even less favorable, in particular, the excess of Mn is 79-fold, Fe—35-fold, Cu—2-fold, and Zn—3–4-fold, which is clearly determined by the closeness of the water basin and the lack of water exchange.

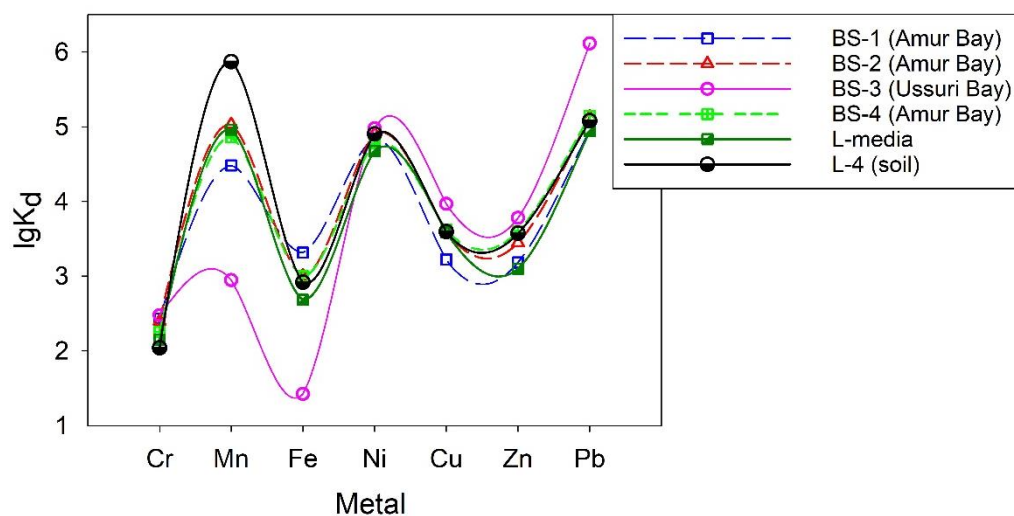
Table 6. The content of the basic metals in the composition of seawater and freshwater bodies.

Marking	Water Area	pH	Li, mg/L	K, mg/L	Na, mg/L	Ca, mg/L	Mg, mg/L	Si, mg/L	Ba, mg/L
W-1	Amur Bay	7.97 ±0.12	148.5 ± 14.1	740.0 ± 70.0	7660.0 ± 720.0	330.0 ± 30.0	1340.0 ± 125.0	440.0 ± 40.0	0.012 ± 0.001
W-3	Ussuri Bay	8.39 ±0.12	160.0 ± 15.2	825.0 ± 78.0	8560.0 ± 810.0	350.0 ± 30.0	1450.0 ± 135.0	1420.0 ± 135.0	0.008 ± 0.001
W-5	Lake Khanka	7.68 ±0.12	1.8 ± 0.2	5.0 ± 0.5	12.0 ± 1.0	17.0 ± 1.0	5.0 ± 0.5	3140.0 ± 300.0	0.048 ± 0.004

Table 7. Content of heavy metals in seawater and freshwater.

Marking	Water Area	Cr, mkg/L	Mn, mkg/L	Fe, mkg/L	Ni, mkg/L	Cu, mkg/L	Zn, mkg/L	Pb, mkg/L
W-1	Amur Bay	<1	24 ± 2	51 ± 4	H/o	66 ± 6	298 ± 25	<1
W-2	Ussuri Bay	<1	7 ± 1	112 ± 10	H/o	50 ± 5	116 ± 10	<1
W-3	Lake Khanka	<1	790 ± 75	3543 ± 325	H/o	165 ± 15	368 ± 30	<1
MPC [46]		≤70	≤10	≤100	≤20	≤100	≤100	≤10
China water quality standard (grade I) [58]		≤50	-	-	-	≤50	≤50	≤10
China water quality standard (grade II) [58]		≤100	-	-	≤25	≤100	≤100	≤5
Japan water quality standard [59]		≤50	-	-	-	≤50	-	≤10
USEPA [60]		≤50	-	≤300	≤20	-	≤5000	≤50
WHO		≤50	≤100	≤100	≤20	-	≤2000	≤50

Figure 10 shows the curves of the dependence of migration and accumulation of HM depending on the metal and the water basin.

**Figure 10.** The rate of HM accumulation in the water–bottom sediment system, depending on the type of metal and the water area.

The interpretation of lgK_d is reduced to the fact that the greater its value, the more intense the process of metal migration from water to bottom sediments is observed. The use of this characteristic within one season enables one to judge the rate of accumulation of a particular metal. In cases when the limits of the seasonal dynamics of HM allows determining the periods of their maximum content in bottom sediments, it is possible to predict the influence of the studied factors on the migration processes of metals in the water–bottom sediments system, which will be carried out and presented in our next study.

Studies have shown that, along with an increase of the pH of the liquid medium (Figure 10), the migration rate decreases with the inverse proportionality of an increase in the accumulation of Cr, Ni, Cu, Zn, and Pb into BS from the aqueous medium. Among other metals, Pb undergoes sedimentation processes into BS most intensively, and the rate generally decreases in the following row: $Pb \gg Mn \geq Ni > Cu > Zn > Fe \gg Cr$. The observed migration pattern for Mn and Ni is moderate.

Despite the increased content of Fe in the seawater and freshwater basins, the distribution coefficient has an almost minimal value, which could indicate the course of competing processes accompanied by the reverse migration of metal from the BS into the water. One of the affecting factors could be a change of pH of the solution in the area of mixing (dilution) of freshwater and seawater, which leads to desorption of cationic forms of HM from the surface of solid particles of suspensions or BS followed by the entry of metals into the water. The greatest effect is observed for the sea samples of Ussuri Bay (Figure 10, BS-3). In natural water, which is a complex multicomponent solution, pH does not depend on the dissociation of its own water molecules, but mainly on the ratio of the amount of carbonic acid and HCO_3^- , CO_3^{2-} , and, to a lesser extent, other ions. It follows that, in addition to the effect of pH on the distribution of HM between components in aquatic ecosystems, the effect of carbonate and bicarbonate ions of natural water must also be taken into account, which requires additional experiments.

4. Conclusions

A correlation between the HM concentration in water, BS, and their migration over the territories under study has been established. It was found that, along with the increase of pH of the liquid medium (freshwater and seawater), the migration rate decreased in reverse proportionality to the accumulation of Cr, Ni, Cu, Zn, and Pb in BS from the liquid medium. The intensity of the deposition process decreases in the following row: $\text{Pb} \gg \text{Mn} \geq \text{Ni} > \text{Cu} > \text{Zn} > \text{Fe} \gg \text{Cr}$. By means of elemental analysis of Lake Khanka coastal soil, multiple surpassing of the contents of some HMs was established that promotes intensification of metal migration into the water and their accumulation in Lake Khanka BS.

It has been determined that BS of both water basins, as well as the Lake Khanka coastal soil, are enriched with Pb and depleted with Cr, Ni, and Zn. In addition, BS of seawater basins are characterized with increased coefficients of Fe and Cu accumulation, unlike freshwater basins, in which the predominant element is Mn. The latter is not reflected in the HM distribution profile, which indicates constant hydrological changes.

The main BS phase composition was determined by the XRD method. It has been demonstrated that the presence of iron oxide in the forms of magnetite and hematite facilitates 'rigid accumulation' of HM preventing their diffusion back into the liquid phase. A direct proportional dependence of the increase of the Ni, Cu, Zn, Fe, and Cr contents on the fraction of iron-oxide and aluminosilicate and carbonate phases preserved over the whole core profile has been established. Analysis of surface BS of seawater areas has demonstrated that the spatial migration elements supplied from the coastal areas is limited and expressed in the decrease of HM concentrations along with removal from the coast. It was shown that, at the transition from the near-estuary (coastal seawater) area of the runoff of the Razdolnaya River to the central one (closer to the outflow to the ocean), the HM concentrations decrease 2–4-fold.

The ecological conditions of the territories under study have been analyzed. According to the calculated values of K_c and I_{geo} of BS of Peter the Great Bay, as regards Cr, Mn, Fe, and Ni, these belong to the class of non-polluted, just like those of Lake Khanka. The main contribution is provided: Cu ($K_c \leq 54.6$), Zn ($K_c \leq 22.2$), and Pb ($K_c \leq 37.2$), whose source includes factory-made effects requiring special attention.

To sum up, the regularities of the spatial distribution of HM in the water areas of Peter the Great Bay and Lake Khanka related to the nonuniform accumulation of Fe and Mn in BS, whose phase carriers are clay fractions and aluminosilicate suspended particles as well as organic substances supplied by the terrigenous runoff, have been established. It has been demonstrated that one can judge, from the gradual increase of contents of Fe, Mn, etc., in BS samples from the near-estuary part to the bay narrow entrance, the effect of the terrigenous runoff on different parts of the water area, with the further determination of the boundaries of possible pollution.

Author Contributions: Conceptualization, E.T. and N.K.; methodology, N.K., A.R., A.E., D.S. and E.T.; formal analysis, E.T. and N.K.; investigation, E.T., N.K., A.R., A.E. and D.S.; data curation, E.T., N.K. and A.R.; writing—original draft preparation, E.T. and N.K.; writing—review and editing, A.E., K.S., X.H. and S.K.; visualization, E.T.; project administration, N.K., X.H. and S.K.; funding acquisition, S.K. and X.H. All authors have read and agreed to the published version of the manuscript.

Funding: The study was supported by the Russian Science Foundation (RSF) (project no. 21-43-00025) and the National Nature Science Foundation of China (NSFC) (project no. 22061132004) as part of an RSF-NSFC cooperation project. Equipment of CUC “Far Eastern Center of Structural Studies” was used in the present work. The work was performed within the framework of the State Order of the Institute of Chemistry, Far Eastern Branch of the Russian Academy of Sciences (project no. FWFN(0205)-2022-0002).

Data Availability Statement: Not applicable.

Acknowledgments: Not applicable.

Conflicts of Interest: The authors declare no conflict of interest.

References

1. Ciparis, S.; Schreiber, M.E.; Voshell, J.R. Using Watershed Characteristics, Sediment, and Tissue of Resident Mollusks to Identify Potential Sources of Trace Elements to Streams in a Complex Agricultural Landscape. *Environ. Monit.* **2012**, *184*, 3109–3126. [CrossRef]
2. Tao, Y.; Yuan, Z.; Xiaona, H.; Wei, M. Distribution and Bioaccumulation of Heavy Metals in Aquatic Organisms of Different Trophic Levels and Potential Health Risk Assessment from Taihu Lake, China. *Ecotoxicol. Environ. Saf.* **2012**, *81*, 55–64. [CrossRef]
3. Campbell, L.M.; Norstrom, R.J.; Hobson, K.A.; Muir, D.C.G.; Backus, S.; Fisk, A.T. Mercury and Other Trace Elements in a Pelagic Arctic Marine Food Web (Northwater Polynya, Baffin Bay). *Sci. Total Environ.* **2005**, *351–352*, 247–263. [CrossRef]
4. Cui, B.; Zhang, Q.; Zhang, K.; Liu, X.; Zhang, H. Analyzing Trophic Transfer of Heavy Metals for Food Webs in the Newly-Formed Wetlands of the Yellow River Delta, China. *Environ. Pollut.* **2011**, *159*, 1297–1306. [CrossRef]
5. Moiseenko, T.I.; Gashkina, N.A. Bioaccumulation of Mercury in Fish as Indicator of Water Pollution. *Geochem. Int.* **2016**, *54*, 485–493. [CrossRef]
6. Monferrán, M.V.; Garnero, P.; de los Angeles Bistoni, M.; Anbar, A.A.; Gordon, G.W.; Wunderlin, D.A. From Water to Edible Fish. Transfer of Metals and Metalloids in the San Roque Reservoir (Córdoba, Argentina). Implications Associated with Fish Consumption. *Ecol. Indic.* **2016**, *63*, 48–60. [CrossRef]
7. Rubio-Franchini, I.; Rico-Martínez, R. Evidence of Lead Biomagnification in Invertebrate Predators from Laboratory and Field Experiments. *Environ. Pollut.* **2011**, *159*, 1831–1835. [CrossRef]
8. Boss, E.; Guidi, L.; Richardson, M.J.; Stemann, L.; Gardner, W.; Bishop, J.K.B.; Anderson, R.F.; Sherrell, R.M. Optical Techniques for Remote and In-Situ Characterization of Particles Pertinent to GEOTRACES. *Prog. Oceanogr.* **2015**, *133*, 43–54. [CrossRef]
9. Man, X.; Huang, H.; Chen, F.; Gu, Y.; Liang, R.; Wang, B.; Jordan, R.W.; Jiang, S. Anthropogenic Impacts on the Temporal Variation of Heavy Metals in Daya Bay (South China). *Mar. Pollut. Bull.* **2022**, *185*, 114209. [CrossRef]
10. Tansel, B.; Rafiuddin, S. Heavy Metal Content in Relation to Particle Size and Organic Content of Surficial Sediments in Miami River and Transport Potential. *Int. J. Sediment Res.* **2016**, *31*, 324–329. [CrossRef]
11. Ali, H.; Khan, E. Bioaccumulation of Non-Essential Hazardous Heavy Metals and Metalloids in Freshwater Fish. Risk to Human Health. *Environ. Chem. Lett.* **2018**, *16*, 903–917. [CrossRef]
12. Radakovitch, O.; Roussiez, V.; Ollivier, P.; Ludwig, W.; Grenz, C.; Probst, J.-L. Input of Particulate Heavy Metals from Rivers and Associated Sedimentary Deposits on the Gulf of Lion Continental Shelf. *Estuarine. Coast. Shelf Sci.* **2008**, *77*, 285–295. [CrossRef]
13. Bradford, W.L.; Luoma, S.N. *Some Perspectives on Heavy Metal Concentrations in Shellfish and Sediment in San Francisco Bay, Contaminants and Sediments, California*; Ann Arbor Science: Ann Arbor, MI, USA, 1980; pp. 501–532. Available online: <https://pubs.er.usgs.gov/publication/70156312> (accessed on 3 June 2023).
14. Daskalakis, K.D.; O'Connor, T.P. Distribution of Chemical Concentrations in US Coastal and Estuarine Sediment. *Mar. Environ. Res.* **1995**, *40*, 381–398. [CrossRef]
15. Hirschberg, D.J.; Chin, P.; Feng, H.; Cochran, J.K. Dynamics of Sediment and Contaminant Transport in the Hudson River Estuary: Evidence from Sediment Distributions of Naturally Occurring Radionuclides. *Estuaries* **1996**, *19*, 931–949. [CrossRef]
16. Dudarev, O.V.; Botsul, A.I.; Savelyeva, N.I.; Charkin, A.N.; Dubina, V.A.; Anikiev, V.V. *Scales of Variability of Lithology and Biochemistry Processes in Estuary of the Razdolnaya River (Sea of Japan): Fluxes of Terrigenous Material and Formation of Bottom Sediments. The State of Marine Ecosystems Affected by River Runoff*; Federal State Unitary Enterprise; Dalnauka: Vladivostok, Russia, 2005; pp. 7–40. (In Russian)
17. Zvalinsky, V.I.; Tishchenko, P.P.; Mikhailik, T.A. *Assessment of the Ecological State of Peter the Great Bay. Current Ecological State of the Peter the Great Bay of the Sea of Japan*; Far Eastern Federal University: Vladivostok, Russia, 2012; pp. 75–113. (In Russian)
18. Shul'kin, V.m. Comparative Assessment of the Aerial and Fluvial Inputs of Matter into Marine Ecosystems. *Geogr. Nat. Resour.* **2012**, *33*, 172–176. [CrossRef]

19. Sevastyanov, A.V.; Lishavskaya, T.S.; Chatkina, T.V. Monitoring of self-purification of sea waters and bottom sediments of the Ussuri Bay in the area of the former landfill for domestic waste (Gornostai Bay). Proceedings of the Federal State Budgetary Institution Far Eastern Regional Research Hydrometeorological Institute. *Vladivostok* **2015**, *S1*, 144–155. (In Russian)
20. Zhuravel, E.V.; Podgurskaya, O.V. Early development of sand dollar *Scaphechinus mirabilis* in the water from different areas of Peter the Great Bay (Japan Sea). *Izvestiya TINRO* **2014**, *178*, 206–216. [\[CrossRef\]](#)
21. Vashchenko, M.A.; Zhadan, P.M.; Almyashova, T.N.; Kovalyova, A.L.; Slinko, E.N. Assessment of the Contamination Level of Bottom Sediments of Amursky Bay (Sea of Japan) and Their Potential Toxicity. *Russ. J. Mar. Biol.* **2010**, *36*, 359–366. [\[CrossRef\]](#)
22. Lukyanova, O.N.; Cherkashin, S.A.; Nigmatulina, L.V.; Chernyaev, A.P.; Veideman, E.L.; Ireykina, S.A.; Pryazhevskaya, T.S. Integral Chemical-Ecological Assessment of the State of Ussuri Bay (the Sea of Japan). *Water Resour.* **2009**, *36*, 615–622. [\[CrossRef\]](#)
23. Ilyichev, V.I.; Karakin, V.P. *Estimation of Severity of Environmental Problems of the Far East Region*; Vestn. USSR Academy of Sciences: Saint Petersburg, Russia, 1988; pp. 84–88. (In Russian)
24. Polyakov, D.M. Long-term variations of heavy metals concentration in the bottom sediments of Amursky Bay. *Vestnik FEB RAS* **2008**, *6*, 134–140. (In Russian)
25. Cherkashin, S.A.; Blinova, N.K. Experimental Studies on the Toxicity of Phenol to Crustacea (Review). *HYD* **2013**, *49*, 61–74. [\[CrossRef\]](#)
26. Losev, O.V. Heavy metals and petroleum hydrocarbons contents in bottom sediments of Uglovoy Bay (Peter the Great Bay, Sea of Japan). *Vestnik FEB RAS* **2020**, *5*, 104–115. (In Russian) [\[CrossRef\]](#)
27. Polyakov, D.M. *Accumulation of Heavy Metals in the Bottom Sediments of the Amur Bay (Sea of Japan)*; Current Ecological State of the Peter the Great Bay of the Sea of Japan; GEOS: Moscow, Russia, 2008; pp. 163–173. (In Russian)
28. Ryumina, A.; Tishchenko, P.; Shkirnikova, E.V. Heavy metals and organic carbon in bottom sediments of shallow bays of Peter the Great Bay. *Geochem. Int.* **2023**, *6*, 1–11. [\[CrossRef\]](#)
29. Kobzar, A.D.; Khristoforova, N.K. Monitoring Heavy-Metal Pollution of the Coastal Waters of Amursky Bay (Sea of Japan) Using the Brown Alga *Sargassum Miyabei* Yendo, 1907. *Russ. J. Mar. Biol.* **2015**, *41*, 384–388. [\[CrossRef\]](#)
30. Kozhenkova, S.I.; Chernova, E.N.; Shulkin, V.M.; Microelement Composition of the Green Alga *Ulva fenestrata* from Peter the Great Bay, Sea of Japan. *Russ. J. Mar. Biol.* **2006**, *32*, 289–296. [\[CrossRef\]](#)
31. Xiang, J. Lake Xingkai/Khanka. Experience and Lessons Learned Brief 2005, International Waters Learning Exchange & Resource Network. 2010, pp. 447–459. Available online: <https://iwlearn.net/documents/5977> (accessed on 3 June 2023).
32. Liu, L.; Feng, Y.; Xu, M.; Xiang, A.; Pan, X.; Xia, X. Effects of Environmental Factors on the Seasonally Change of Chlorophyll-a in Eutrophic Plateau Lake Dianchi, China. In Proceedings of the 2012 International Conference on Biomedical Engineering and Biotechnology, Macau, China, 28–30 May 2012; pp. 1401–1403. [\[CrossRef\]](#)
33. Simokon, M.V.; Kovekovdova, L.T.; Narevich, I.S. Trace elements in water quality assessment of Lake Khanka. *Tihookean. Geogr.* **2021**, *3*, 64–74. [\[CrossRef\]](#)
34. Kovekovdova, L.T.; Simokon, M.V. Tendencies in change of chemoecological situation in the coastal area of Primorye. Toxic elements in bottom sediments and aquatic organisms. *Izvestiya TINRO* **2004**, *137*, 310–320. (In Russian)
35. Chernova, A.S.; Lishavskaya, T.S.; Sevastyanov, A.V. Concentrations of contaminants in Peter the Great Bay (Japan Sea) in 2004–2008. *Izvestiya TINRO* **2011**, *164*, 330–339. (In Russian)
36. Petukhov, V.I.; Petrova, E.A.; Losev, O.V. Heavy metals and oil products in the waters of the Uglovoy Bay (Amur Bay, Sea of Japan) in the warm and cold periods of the year. *Vestnik FEB RAS* **2018**, *1*, 85–93. (In Russian)
37. Sun, W.; Zhang, E.; Liu, E.; Chang, J.; Shen, J. Linkage between Lake Xingkai Sediment Geochemistry and Asian Summer Monsoon since the Last Interglacial Period. *Palaeogeogr. Palaeoclimatol. Palaeoecol.* **2018**, *512*, 71–79. [\[CrossRef\]](#)
38. Grabenko, E.A.; Bukin, I.O.; Kuzmenkova, N.V. Lake drill modernization for sampling the undisturbed marine and lake sediment with different composition. *Geol. Geogr. Glob. Energy* **2022**, *4*, 122–130. [\[CrossRef\]](#)
39. Abril, J.M. On the Use of ²¹⁰Pb-Based Records of Sedimentation Rates and Activity Concentrations for Tracking Past Environmental Changes. *J. Environ. Radioact.* **2022**, *244–245*, 106823. [\[CrossRef\]](#)
40. Ito, E.; Miura, S.; Aoyama, M.; Shichi, K. Global ¹³⁷Cs Fallout Inventories of Forest Soil across Japan and Their Consequences Half a Century Later. *J. Environ. Radioact.* **2020**, *225*, 106421. [\[CrossRef\]](#)
41. Hakanson, L. An Ecological Risk Index for Aquatic Pollution Control: A Sedimentological Approach. *Water Res.* **1980**, *14*, 975–1001. [\[CrossRef\]](#)
42. Muller, G. Index of geoaccumulation in sediments of the Rhine River. *Geo J. Libr.* **1969**, *2*, 108–118.
43. Vinogradov, A.P. Patterns of distribution of chemical elements in the earth's crust. *Geochem. Int.* **1956**, *1*, 6–52. (In Russian)
44. Muller, G. The heavy metal pollution of the sediments of Neckars and its tributary: A stocktaking. *Chem. Zeit.* **1981**, *105*, 157–164.
45. Tessier, A.; Campbell, P.G.C.; Bisson, M. Trace Metal Speciation in the Yamaska and St. François Rivers (Quebec). *Can. J. Earth Sci.* **1980**, *17*, 90–105. [\[CrossRef\]](#)
46. GN 2.1.5.1315-03—MPC of Chemical Substances in the Water of Water Objects for Household and Drinking and Cultural and Household Water Use. 2003. Available online: <http://www.dioxin.ru/doc/gn2.1.5.1315-03.htm> (accessed on 3 June 2023).
47. Shulkin, V.M. *Metals in Ecosystems of Marine Shallow Waters*; Dalnauka: Vladivostok, Russia, 2004; 279p. (In Russian)
48. Aung, P.P.; Mao, Y.; Hu, T.; Qi, S.; Tian, Q.; Chen, Z.; Xing, X. Metal Concentrations and Pollution Assessment in Bottom Sediments from Inle Lake, Myanmar. *J. Geochem. Explor.* **2019**, *207*, 106357. [\[CrossRef\]](#)

49. Krinochkin, L.A. Regional geochemical mapping as a basis for assessing the mineragenic potential of the Russian subsoil. *J. Explor. Prot. Subsoil* **2016**, *11*, 6–13. (In Russian)
50. Anikeev, V.V.; Dudarev, O.V.; Kasatkina, A.P.; Kolesov, G.M. Influence of terrigenous and biogenic factors on the formation of sedimentary fluxes of chemical elements in the coastal zone of the Sea of Japan. *Geochem. Int.* **1996**, *1*, 59–72. (In Russian)
51. Astakhov, A.S.; Kalugin, I.A.; Aksentov, K.I.; Dar'in, A.V. Geochemical indicators of paleo-typhoons in shelf sediments. *Geochem. Int.* **2015**, *53*, 383–388. [[CrossRef](#)]
52. Kuzmenkova, N.; Rozhkova, A.; Egorin, A.; Tokar, E.; Grabenko, E.; Shi, K.; Petrov, V.; Kalmykov, S.; Hou, X. Analysis of Sedimentation Processes in Lake Khanka (Xingkaihu) and Amur Bay Using ¹³⁷Cs and ²¹⁰Pbex Tracers. *J. Radioanal. Nucl. Chem.* **2023**, *332*, 959–971. [[CrossRef](#)]
53. Goncharuk, V.V.; Yakimova, T.I. The use of substandard groundwater in drinking water supply. *Chem. Technol. Water* **1996**, *18*, 495–529. (In Russian)
54. Gavrilova, I.P.; Kasimov, N.S. *Workshop on Landscape Geochemistry*; Moscow University: Moscow, Russia, 1989; 72p.
55. Zemskova, L.; Egorin, A.; Tokar, E.; Ivanov, V.; Bratskaya, S. New Chitosan/Iron Oxide Composites: Fabrication and Application for Removal of Sr²⁺ Radionuclide from Aqueous Solutions. *Biomimetics* **2018**, *3*, 39. [[CrossRef](#)] [[PubMed](#)]
56. Khanchuk, A.I.; Ratkin, V.V.; Ryazantseva, M.D.; Golozubov, V.V.; Gonokhova, N.G. *Geology and Minerals of the Primorsky Region*; Dalnauka: Vladivostok, Russia, 1995; 57p. (In Russian)
57. Maldonado, M.T.; Hughes, M.P.; Rue, E.L.; Wells, M.L. The Effect of Fe and Cu on Growth and Domoic Acid Production by Pseudo-Nitzschia Multiseries and Pseudo-Nitzschia Australis. *Limnol. Oceanogr.* **2002**, *47*, 515–526. [[CrossRef](#)]
58. GB3838-2002; Environmental Quality Standards for Surface Water. Ministry of Ecology and Environment: Beijing, China, 2002.
59. Ministry of the Environment Government of Japan, Conservation of the Water Environment—Chapter 3. Available online: <https://www.env.go.jp/en/water/wq/wemj/water.html> (accessed on 3 June 2023).
60. USEPA. *Using Stressor-Response Relationships to Derive Numeric Nutrient Criteria*; Environmental Protection Agency, Office of Water: Washington, DC, USA, 2010.

Disclaimer/Publisher's Note: The statements, opinions and data contained in all publications are solely those of the individual author(s) and contributor(s) and not of MDPI and/or the editor(s). MDPI and/or the editor(s) disclaim responsibility for any injury to people or property resulting from any ideas, methods, instructions or products referred to in the content.